

## THREE

# The SPICE Diode Model

### Special Acknowledgment

This chapter was written by Howard T. Russell, Jr., PhD, OPAL Engineering, Inc., August 4, 1991, under contract with Motorola Inc. Opal Engineering is located at 828 Opal Drive, Suite 1, San Jose, CA 95117.

### Introduction

This chapter presents a description of the SPICE diode model and methods for the extraction of its parameters. A comprehensive examination of this model will be given along with comparisons of the characteristics of a real diode and those produced by the model. These comparisons will be used to illustrate the model's accuracy and limitations. Based on the nature of the model equations, mathematical methods for the extraction of the SPICE parameters (with the exception of the noise parameters) will be presented. These methods are easily implemented on a hand-held programmable calculator and will be used to extract the parameters for a Motorola MURH840CT rectifier as an example. Throughout this chapter, references are made to the characteristics and behavior of an ideal diode model. The development of this model may be found in several of the many well-known texts on the subjects of semiconductor device theory and *pn* junction diodes [1–4].

The SPICE model of a *pn* junction diode consists of mathematical equations, parameters, and variables, all of which are designed to work together to simulate as accurately as possible the electrical characteristics of a real device. The equations and variables used for the model in the SPICE program are fixed and not easily modified [5, 6]. Therefore, the accuracy resulting from a SPICE simulation of a diode depends on the precise extraction of its model parameters. Fortunately, there are several parameter extraction methods which can be applied to this model, some of which yield more accurate results than others. The inherent success of a particular method depends for the most part on how well device physics and theory are utilized in the design of the model, and upon the availability of data taken from a real device.

### The SPICE Diode Model

The parameters for the SPICE model of the diode are given in Table 3.1 [5, 6]. The equations that use these parameters are divided into four model groups which are responsible for simulating various diode characteristics. These groups consist of the

TABLE 3.1 SPICE Diode Model Parameters

Name	Parameter	Default value	Typical value	Units
IS	Saturation current	10.0f	50.0f	A
RS	Ohmic resistance	0	2.0	ohm
N	Emission coefficient	1.0	1.1	
TT	Forward transit time	0	10.0n	sec
CJO	Zero-bias junction capacitance	0	10.0p	F
VJ	Contact potential	1.0	0.8	V
M	Junction capacitance grading exponent	0.5	0.3	
EG	Energy gap	1.11	1.11	eV
XTI	IS temperature exponent	3.0	3.0	
KF	Flicker noise coefficient	0	0.1f	
AF	Flicker noise exponent	1.0	1.0	
FC	CJ forward-bias coefficient	0.5	0.5	
BV	Reverse breakdown	$\infty$	100.0	V
IBV	Current at BV	1.0m	200.0p	A

large-signal dc model, the small-signal ac model, temperature and area effects, and the noise model.

**The Large-signal DC Model.** The large-signal behavior of the SPICE diode is characterized by the relationship between the dc current and voltage at its terminals. The parameters used to model this behavior are IS, RS, N, BV, and IBV. The parameter IS is the same as the reverse saturation current  $I_s$  for an ideal diode. The ohmic resistance RS is used to model the resistance of the metal contacts and the neutral regions under high-level injection. The emission coefficient N is used to modify the slope of the current versus voltage (I-V) characteristics curve. Finally, the parameters BV and IBV model the reverse breakdown behavior.

Figure 3.1 shows the equivalent circuit of the SPICE diode for large-signal dc analysis. This circuit contains an internal diode  $D_1$ , a series resistance having a value

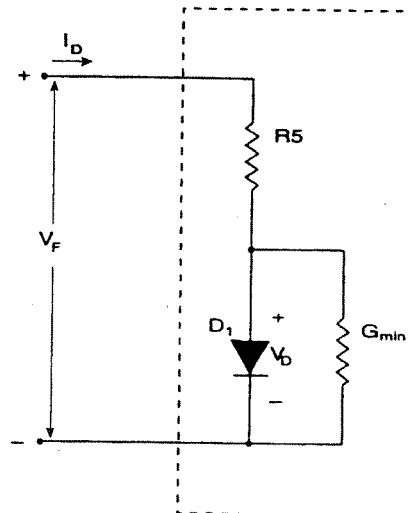


FIGURE 3.1 DC Large-signal SPICE Diode Model.

of  $R_S$ , and a shunt conductance  $G_{MIN}$ . The SPICE program adds this conductance, which is transparent to the user, around every internal  $pn$  junction to aid convergence. The program default value for  $G_{MIN}$  is  $10^{-12}$  mhos but can be set to any other non-zero value with a .OPTIONS line in the circuit file [5].

The dc model variables consist of the voltage across the external diode terminals  $V_F$ , the voltage across the internal diode terminals  $V_D$ , and the terminal current  $I_D$ . With these parameters and variables, the large-signal dc characteristics are modeled by the following equations

$$V_F = R_S \cdot I_D + V_D \quad (3.1)$$

and

$$I_D = f(V_D) \quad (3.2)$$

where four regions of operation describe the functional relationship between the internal diode voltage and diode current.

(a) For  $V_D \geq -5 \cdot N \cdot V_t$

$$I_D = IS \cdot \left\{ \exp\left(\frac{V_D}{N \cdot V_t}\right) - 1 \right\} + G_{MIN} \cdot V_D \quad (3.3)$$

(b) For  $-BV < V_D < -5 \cdot N \cdot V_t$

$$I_D = -IS + G_{MIN} \cdot V_D \quad (3.4)$$

(c) For  $V_D = -BV$ ,

$$I_D = -IBV \quad (3.5)$$

(d) For  $V_D < -BV$ ,

$$I_D = -IS \cdot \left\{ \exp\left(\frac{-(BV + V_D)}{V_t}\right) - 1 + \frac{BV}{V_t} \right\} \quad (3.6)$$

For all of these equations,  $V_t$  is the *thermal voltage* which is defined as

$$V_t = \frac{k \cdot T}{q} \quad (3.7)$$

To insure convergence between regions (c) and (d), it is necessary that  $IBV$  is defined as

$$IBV \geq \frac{IS \cdot BV}{V_t} \quad (3.8)$$

A typical plot of  $I_D$  versus  $V_D$  generated by these equations is shown in Figure 3.2 where each of the regions (a) through (d) are indicated.

### The Small-Signal AC Model

The ac model of the SPICE diode is derived from the linearized small-signal behavior of the internal diode  $D_1$  shown in Figure 3.1. The circuit elements of this model

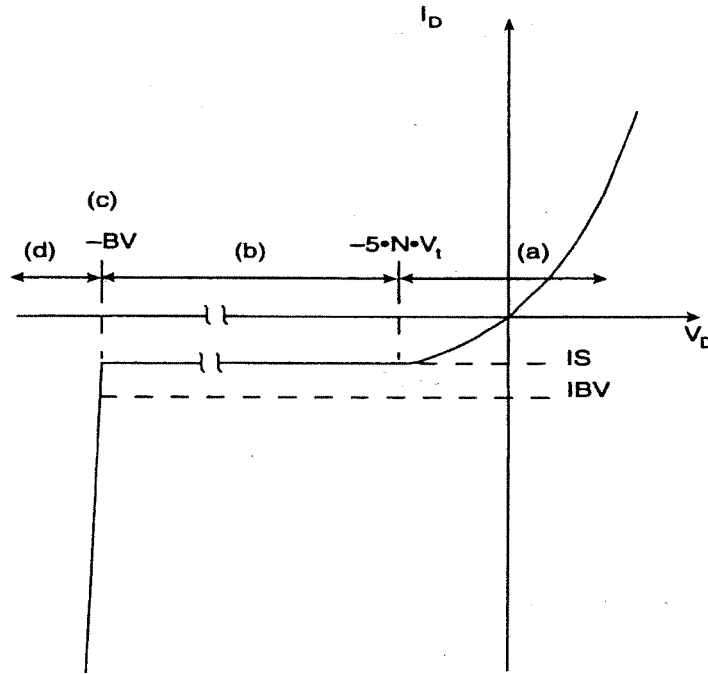


FIGURE 3.2 Large-scale I-V Characteristics of the SPICE Diode Model.

include the junction capacitance  $CJ$ , the dynamic conductance  $GD$ , and the diffusion capacitance  $CD$ , all of which are bias dependent as are those corresponding elements of the ideal diode model.

The junction capacitance is modeled by the parameters  $CJO$ ,  $VJ$ ,  $M$ , and  $FC$ . The parameters  $CJO$  and  $VJ$  are identical to the zero-bias junction capacitance  $C_j(0)$  and the contact potential  $V_j$  described for an ideal diode. The parameter  $M$  is a grading exponent that is used to change the slope of the junction capacitance versus voltage (C-V) characteristics curve. For abrupt or step junctions,  $M$  is 0.5 while for linearly graded junctions,  $M$  is about 0.333. The parameter  $FC$  is used to model the capacitance under forward bias conditions.

The variables for the model are the junction capacitance  $CJ$  in farads and the internal diode voltage  $V_D$  which are related by

$$CJ = f(V_D) \quad (3.9)$$

where two regions of operation describe this function.

(a) For  $V_D < FC \cdot VJ$ ,

$$CJ = CJO \cdot \left\{ 1 - \frac{V_D}{VJ} \right\}^{-M} \quad (3.10)$$

(b) For  $V_D \geq FC \cdot VJ$ ,

$$CJ = \frac{CJO}{(1 - FC)^{(M+1)}} \cdot \left( 1 - FC \cdot (M+1) + \frac{M \cdot V_D}{VJ} \right) \quad (3.11)$$

To insure that the last equation remains well behaved, FC is restricted to values between zero and one; that is,

$$0 \leq FC < 1 \quad (3.12)$$

A typical C-V curve produced by these equations is shown in Figure 3.3 where each of the two regions are indicated.

The dynamic conductance is modeled by the slope of the I-V curve evaluated at a particular bias voltage. This slope is found from the voltage derivative of the current described in equations (3.3) through (3.6). The conductance GD in mhos of the internal diode  $D_1$  as a function of the voltage  $V_D$  is derived from

$$GD = f(V_D) \quad (3.13)$$

where three regions of operation describe this functional relationship which involve the parameters IS and N.

(a) For  $V_D \geq -5 \cdot N \cdot V_t$ ,

$$GD = \left( \frac{IS}{N \cdot V_t} \right) \cdot \exp\left( \frac{V_D}{N \cdot V_t} \right) \quad (3.14)$$

(b) For  $-BV < V_D < -5 \cdot N \cdot V_t$ ,

$$GD = -\frac{IS}{V_D} \quad (3.15)$$

(c) For  $V_D \leq -BV$ ,

$$GD = 0 \quad (3.16)$$

The diffusion capacitance CD is modeled by the forward transit time parameter TT, and the parameters IS and N. Similar to an ideal diode, this capacitance in farads is voltage dependent and is derived from

$$CD = f(V_D) \quad (3.17)$$

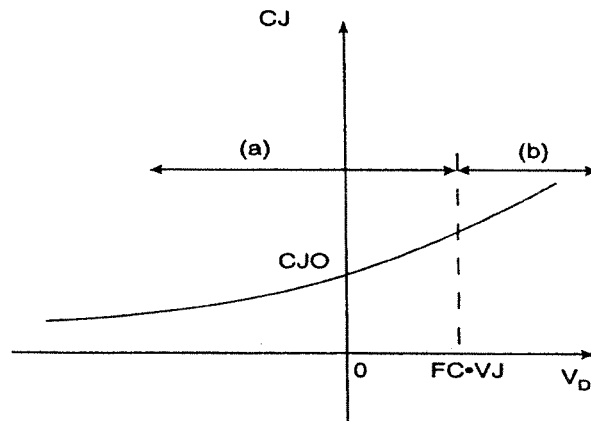


FIGURE 3.3 Junction C-V Characteristics of the SPICE Diode Model.

where three regions of operation describe this functional relationship:

(a) For  $V_D \geq -5 \cdot N \cdot V_i$ ,

$$CD = \left( \frac{TT \cdot IS}{N \cdot V_i} \right) \cdot \exp\left( \frac{V_D}{N \cdot V_i} \right) \quad (3.18)$$

(b) For  $-BV < V_D < -5 \cdot N \cdot V_i$ ,

$$CD = -\frac{TT \cdot IS}{V_D} \quad (3.19)$$

(c) For  $V_D \leq -BV$

$$CD = 0 \quad (3.20)$$

The complete small-signal ac model of the SPICE diode is shown in Figure 3.4 where the resistance  $RS$  has been included with the elements defined above.

### Temperature and Area Effects

Temperature behavior of the SPICE diode is modeled through certain temperature-dependent parameters. These parameters are  $IS$ ,  $VJ$ ,  $CJO$ , and  $FC$ . In the equations to follow,  $TNOM$  is the nominal or reference temperature having a default value of  $27^\circ\text{C}$ . This value can also be changed with the use of the `.OPTIONS` line. The variable  $T$  is the analysis temperature (in  $^\circ\text{C}$ ) which has a default value of  $27^\circ\text{C}$  if the `.TEMP` line is omitted from the circuit file. If the `.TEMP` line is used for temperature analysis,  $T$  takes on the values given in this line. It is important to note that SPICE assumes all input data and model parameters have been specified at  $27^\circ\text{C}$ . Even though temperature is specified in the circuit file and in the `.OPTIONS` line in  $^\circ\text{C}$ , it is converted by SPICE to  $^\circ\text{K}$  for use in the equations.

For the saturation current  $IS$ , the parameters  $N$ ,  $EG$ , and  $XTI$  are used to model its temperature dependence with the equation

$$IS(T) = IS(TNOM) \cdot \left( \frac{T}{TNOM} \right)^{XTI/N} \cdot \exp\left\{ \left[ \frac{q \cdot EG}{N \cdot k} \right] \cdot \left[ \frac{1}{TNOM} - \frac{1}{T} \right] \right\} \quad (3.21)$$

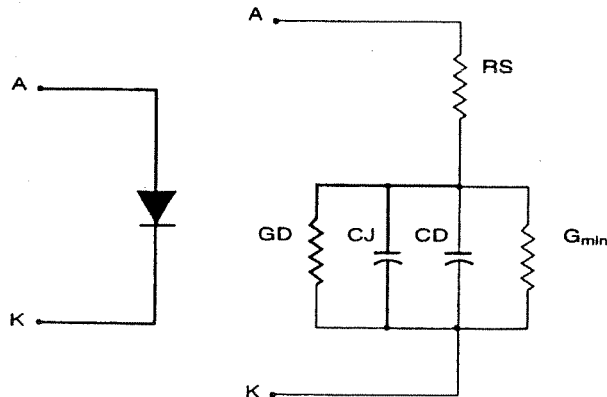


FIGURE 3.4 AC Small-signal SPICE Diode Model.

where  $IS(TNOM)$  is the nominal value of the saturation current and  $IS(T)$  is the value evaluated at the analysis temperature  $T$ .

The contact potential  $VJ$  has the temperature-dependent function given below

$$VJ(T) = VJ(TNOM) \cdot \left( \frac{T}{TNOM} \right) + \frac{2 \cdot k \cdot T}{q} \cdot \ln \left( \frac{n_i(TNOM)}{n_i(T)} \right) \quad (3.22)$$

In this expression,  $VJ(TNOM)$  is the  $TNOM$  value of  $VJ$ ,  $VJ(T)$  is the value evaluated at  $T$ , and  $n_i(T)$  is the intrinsic carrier concentration (in  $\text{cm}^{-3}$ ) of silicon which is also a function of temperature. That is,

$$n_i(T) = 1.45 \cdot 10^{10} \cdot \left( \frac{T}{TNOM} \right)^{1.5} \times \exp \left\{ \left[ \frac{q}{2 \cdot k} \right] \cdot \left[ \frac{E_g(TNOM)}{TNOM} - \frac{E_g(T)}{T} \right] \right\} \quad (3.23)$$

where  $E_g(T)$  is the temperature-dependent function for the energy gap (in eV) of silicon. From experimental results, this function is found to be

$$E_g(T) = 1.16 - \frac{7.02 \cdot 10^{-4} \cdot T^2}{T + 1108.0} \quad (3.24)$$

At  $27^\circ\text{C}$ ,  $E_g$  calculates to be about 1.115 eV.

For the zero-bias junction capacitance  $CJO$ , the parameters  $M$  and  $VJ$  are used to model its temperature dependence with the equation:

$$CJO(T) = CJO(TNOM) \cdot \left\{ 1 + 4 \cdot 10^{-4} \cdot M \cdot (T - TNOM) + m \cdot \left[ 1 - \frac{VJ(T)}{VJ(TNOM)} \right] \right\} \quad (3.25)$$

The last temperature-dependent parameter is  $FC$ , the junction capacitance forward-bias coefficient. This parameter has the simple function given as:

$$FC(T) = FC(TNOM) \cdot \left( \frac{VJ(T)}{VJ(TNOM)} \right) \quad (3.26)$$

For the ideal diode, certain parameters are functions of the junction area. The SPICE program also provides area-dependency on these parameters through the use of the  $AREA$  factor in the diode description line in the circuit file. The parameters affected by the  $AREA$  factor are  $IS$ ,  $RS$ ,  $CJO$ , and  $IBV$  which are modified by the following equations:

$$IS = AREA \cdot IS \quad (3.27)$$

$$RS = \frac{RS}{AREA} \quad (3.28)$$

$$CJO = AREA \cdot CJO \quad (3.29)$$

$$IBV = AREA \cdot IBV \quad (3.30)$$

where  $AREA$  has a default value of 1.

### The Noise Model

Small-signal noise behavior of the SPICE diode is modeled by two noise current sources added to the small-signal ac circuit model as shown in Figure 3.5. The current source  $i_{RS}$  is responsible for modeling thermal noise generated by the resistance  $R_S$ . The mean-squared value of thermal noise current (in  $A^2$ ) generated by this source is expressed as

$$\overline{i_{RS}^2} = \frac{4 \cdot k \cdot T}{R_S} \cdot \Delta f \quad (3.31)$$

where  $T$  is the temperature in  $^{\circ}K$  and  $\Delta f$  is the noise bandwidth in Hz. The current source  $i_D$  is responsible for modeling both shot and flicker noise ( $1/f$  noise) generated in the depletion region of the diode. The total mean-squared value of noise current (in  $A^2$ ) generated by this source is expressed as

$$\overline{i_D^2} = 2 \cdot q \cdot I_D \cdot \Delta f + KF \cdot \frac{I_D^{AF}}{f} \cdot \Delta f \quad (3.32)$$

where  $I_D$  is the dc diode current,  $f$  is the frequency at which the noise is measured, and  $AF$  and  $KF$  are SPICE flicker noise parameters.

### The Diode Model versus a Real Diode

To see how well the equations for the SPICE diode model simulate the behavior of both ideal and real diodes, comparisons are made among the terminal characteristics of all three. These comparisons use standard characteristic curves which illustrate the behavior of a typical real diode (shown with solid curves), and those produced by the ideal and SPICE diode models (shown with dashed curves). For clarity, all curves are labeled to indicate their origin.

The current (logarithmic scale) versus voltage (linear scale) for a diode driven by a forward-bias dc voltage is plotted and shown in Figure 3.6. From this I-V plot,

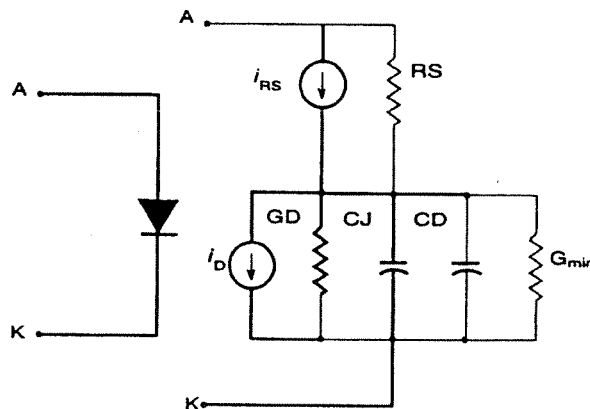


FIGURE 3.5 AC Small-signal SPICE Diode Model with Noise Sources.



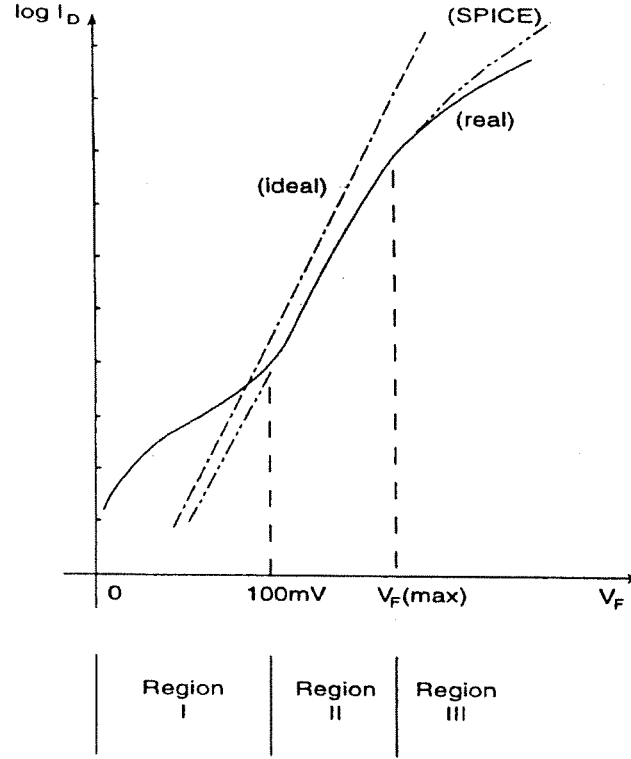


FIGURE 3.6 Forward-bias I-V Characteristics for the Real, Ideal, and SPICE Diodes.

three distinct regions of operation are observed. In Region I, the device is operating under *extreme low-level injection* for bias voltages ranging from zero to about 100 mV, typically. For this mode of operation, the injected carriers passing through the depletion region are largely affected by the many generation and recombination (G-R) centers found near the metallurgical junction. The dominant effect of these G-R centers causes the increase in the diode current with respect to the voltage to be smaller than ideally predicted. In Region II, the diode is operating under *low-level injection*. The voltage range for this region is from about 100 mV to a value determined by  $V_F(\text{max})$  which is derived from

$$V_F(\text{max}) = V_i \cdot \ln \left( \frac{N_{\text{low}}^2}{10 \cdot n_i^2} \right) \quad (3.33)$$

where  $N_{\text{low}}$  is the smaller of the impurity concentrations. Under this mode of operation, the G-R centers do not affect the injected carriers as much as in Region I, and the current increase over this voltage range is found to be close to that predicted for an ideal diode. Beyond the voltage  $V_F(\text{max})$ , the diode operates under *high-level injection* as illustrated by Region III. Here the resistances of the neutral  $n$  and  $p$ -type regions produce ohmic voltage drops which tend to reduce the current increase. As these drops become more dominant, the diode current stops increasing exponentially and becomes more proportional to the bias voltage.

Superimposed on this plot is the dashed curve representing the I-V characteristics of an ideal diode. It is clear that this model is fairly accurate in Region II, but falls short of predicting the behavior of Regions I and III. The second dashed curve is that of the SPICE diode which is generated by Equations 3.1 and 3.3. Compared to the real diode, the characteristics produced by this model illustrate significant accuracy in Regions II and III. However, like the ideal diode, the characteristics are less accurate in Region I.

In Figure 3.7, the linear-scaled I-V characteristics of a real diode are shown for both the forward and reverse-bias conditions. As the reverse-bias voltage increases toward the breakdown voltage, the diode current in the reverse direction exhibits a slight increase due to surface leakage effects. For real diodes, this current is referred to as the *reverse leakage current*  $I_R$ . The current at which breakdown occurs is called the *breakdown current*  $I_{BV}$ . The first dashed curve represents the I-V characteristics of an ideal diode. Under reverse-bias conditions, the reverse leakage current is maintained by the saturation current  $I_S$  which is constant and not affected by the voltage. Even though the breakdown voltage can be calculated, the true breakdown behavior is not predicted by the ideal diode model equations.

The second dashed curve represents the I-V characteristics of the SPICE diode as generated by Equations 3.3 through 3.6. For this model, the reverse leakage current is maintained by the saturation current parameter  $I_S$ , which is also constant and unaffected by the voltage. However, the behavior of the model at the breakdown voltage is fairly close to that of a real diode.

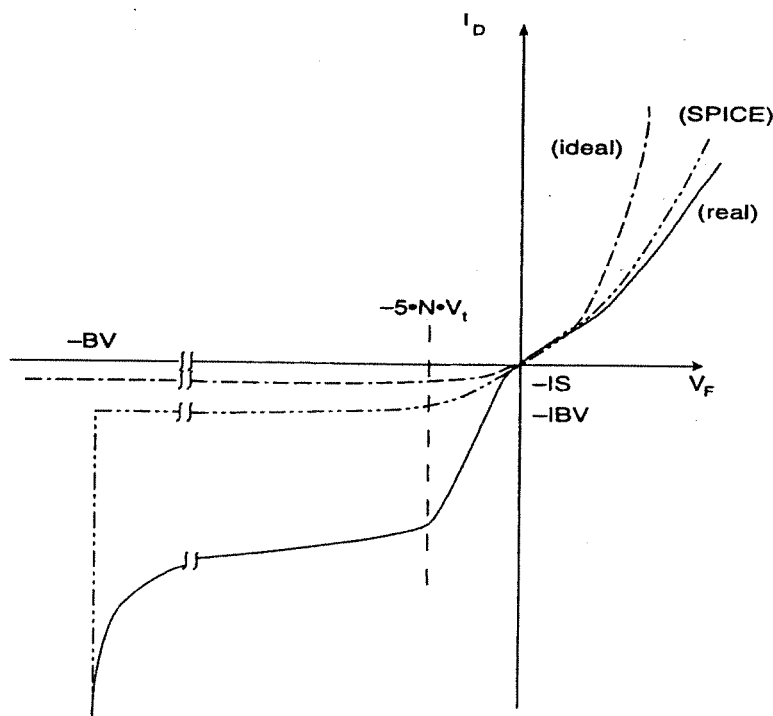
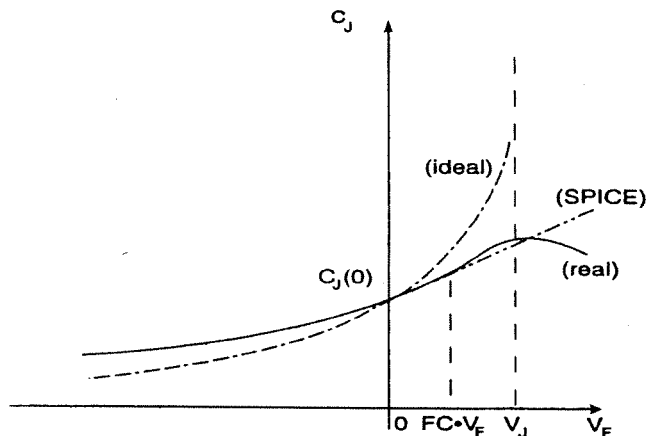


FIGURE 3.7 Forward and Reverse-bias I-V Characteristics for the Real, Ideal, and SPICE Diodes.

Junction capacitance versus voltage characteristic curves are shown in Figure 3.8. Under forward-bias, the C-V characteristics for a real diode are well behaved for voltage values close to the contact potential  $V_j$ . For an ideal diode, however, the capacitance calculated near  $V_j$  tends to approach unrealistic values. In the reverse-bias region, the results of this equation show close similarity to the capacitance of a real diode.

The results of the SPICE diode junction capacitance equations show a very accurate similarity to the capacitance of a real diode, especially in the reverse-bias region. This is due in part to the parameter  $M$  in Equation 3.10 which allows the slope of the C-V curve to vary. In the forward-bias region, the parameter  $FC$  is used in Equation 3.11 to produce a straight-line approximation to the C-V curve for voltages beyond  $FC \cdot V_j$ .

A plot of diffusion capacitance as a function of forward-bias diode current is shown in Figure 3.9. The diffusion capacitance behavior of an ideal diode illustrates



**FIGURE 3.8** Forward and Reverse-bias Junction C-V Characteristics for the Real, Ideal, and SPICE Diodes.

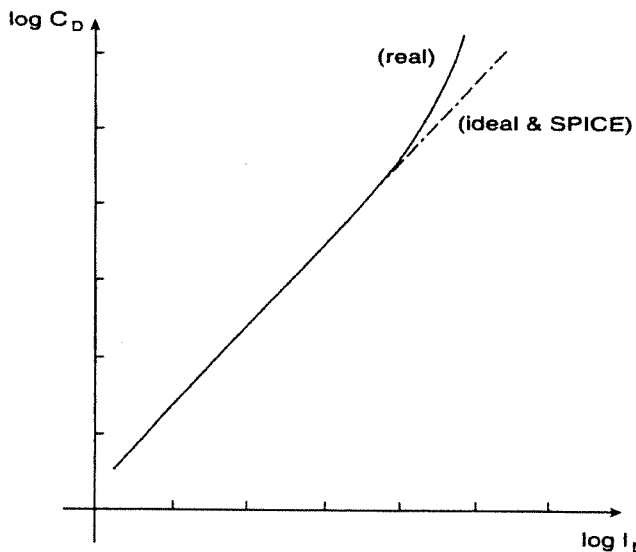


**FIGURE 3.9** Diffusion Capacitance Characteristics for the Real, Ideal, and SPICE Diodes.

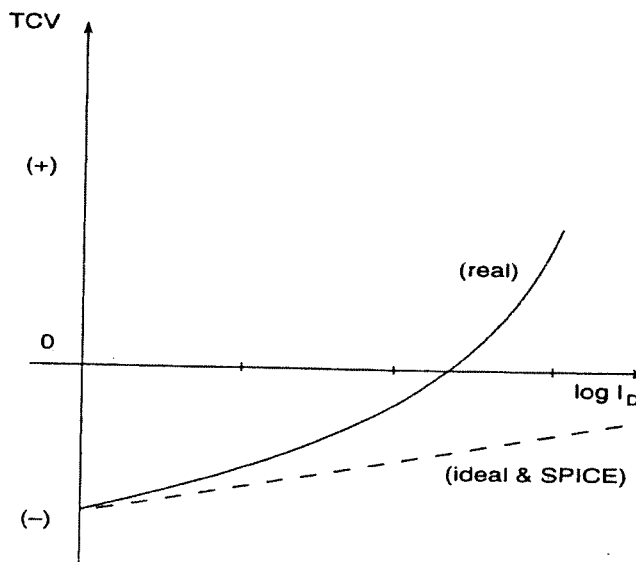
a proportional increase in capacitance with current since the forward transit time  $\tau_T$  is assumed to be constant. This is the case for the SPICE diode since the corresponding parameter  $TT$  is also constant. For a real diode, however,  $\tau_T$  is known to increase with current at high current levels due to current crowding effects. Thus, the diffusion capacitance typically deviates from predicted behavior as illustrated.

Figure 3.10 is a plot of the voltage temperature coefficient (TCV) as a function of forward-bias current. The TCV for a real diode typically has negative values over low current ranges but increases to positive values at higher currents. This is due mainly to the positive temperature coefficient of the bulk resistance which dominates the diode voltage at these levels. The TCV of an ideal diode has negative values over a large range of current as shown. This is also true for the SPICE diode since the resistance parameter  $RS$  has no temperature coefficient.

### SPICE Diode Model Parameter Limitations and Restrictions

Based on these comparisons, it is obvious that the SPICE diode model is capable of performing a fairly accurate job in simulating the behavior of a real  $pn$  junction diode. It is just as obvious, however, that the model is also limited in its range of accurate simulation due in part to limitations of its parameters. The following statements provide a review of the limitations on the model parameters and how they affect the simulation results. For some of the parameters, suggested value restrictions are given in order to insure convergence.

- (a) The saturation current  $I_S$  is constant and not a function of the reverse-bias voltage. Therefore, the simulated reverse leakage current remains constant over the reverse-bias region up to the breakdown voltage.



**FIGURE 3.10** Voltage Temperature Coefficient (TCV) Characteristics for the Real, Ideal, and SPICE Diodes.

- (b) The ohmic resistance  $R_S$  is constant and not a function of current or voltage. The resistance of the bulk neutral semiconductor regions of a real diode actually increases as current increases for high-level injection.
- (c)  $R_S$  has no temperature coefficient. The temperature coefficient of the resistance of the bulk neutral semiconductor regions of a real diode is actually positive, which produces a positive TCV at high-level injection.
- (d) The emission coefficient  $N$  is constant, and cannot model the change in the slope of the I–V characteristics between the extreme low-level and low-level injection regions. For convergence purposes,  $N$  must be greater than 0.01.
- (e) The forward transit time  $TT$  is constant and not a function of current or voltage. As such, the diffusion capacitance  $CD$  will increase proportionally with current and the simulated reverse recovery time  $t_r$  will be constant over current.
- (f) The temperature dependence of the zero-bias junction capacitance  $CJO$  is consistent with that of silicon only. In Equation 3.25, the coefficient of thermal expansion is that of silicon material.
- (g) From Equations 3.22 to 3.24, the  $TNOM$  value of the contact potential  $VJ$  must be greater than 0.4 V to insure convergence for temperature analysis up to 200°C. For a larger value of the analysis temperature, these equations can be used to determine the minimum value of  $VJ$ .
- (h) The temperature dependencies of the contact potential  $VJ$ , the intrinsic carrier concentration  $n_i$ , and the energy gap  $EG$  given in Equations 3.22 to 3.24, respectively, are consistent with that of silicon material only.
- (i) For convergence, the forward bias coefficient  $FC$  is restricted to values between zero and one as indicated in Equation 3.12; that is,

$$0 \leq FC < 1.0.$$

- (j) The reverse breakdown voltage  $BV$  has a default value of infinite. A specified value of zero for  $BV$  is interpreted by SPICE to mean infinite.
- (k) The reverse breakdown characteristics of a real diode tend to be “soft”; that is, the reverse leakage current gradually increases toward the breakdown current as the reverse-bias voltage increases. For the SPICE model, the reverse leakage current is modeled by the parameter  $IS$  which is constant out to the breakdown voltage. This produces a “hard” breakdown characteristic for the model.
- (l) The current at the breakdown voltage  $IBV$  is dependent upon  $IS$  and  $BV$ . For convergence,  $IBV$  is restricted to values determined by

$$IBV \geq \frac{IS(T) \cdot BV}{V_t(T)} \quad (3.34)$$

where the saturation current  $IS$  and the thermal voltage  $V_t$  must be calculated at the largest value of simulation temperature by Equations 3.21 and 3.7, respectively.

- (m)  $IBV$  is often not consistent with the breakdown current  $I_{BV}$  of a real diode at the specified breakdown voltage.

## SPICE Diode Model Parameter Extraction Methods

The methods given in this section for the extraction of the SPICE diode model parameters are based on data acquired from a real device. Table 3.2 lists the necessary data required for the extraction of certain parameters. This data may be taken from actual

**TABLE 3.2** Diode Data Requirements for SPICE Model Parameter Extraction

Data Required	Parameters Extracted
Forward dc characteristics; forward diode current ( $I_D$ ) versus forward diode voltage ( $V_F$ ).	IS, RS, N
Junction capacitance characteristics; reverse-bias junction capacitance ( $C_j$ ) versus reverse bias voltage ( $V_R$ ).	CJO, VJ, M
Reverse recovery time ( $t_r$ ) versus forward diode current ( $I_F$ ).	TT
Forward voltage ( $V_F$ ) temperature coefficient versus forward current ( $I_D$ ), or reverse current ( $I_R$ ) versus temperature.	EG, XTI
Breakdown voltage characteristics.	BV, IBV
Noise measurements (parameters usually set to default values).	KF, AF
Other parameters for which the defaults are assumed: FC = 0.5 (typical)	FC

measurements or from characteristic plots available on most data sheets. For data sheet information, it is assumed that the plots represent a typical device and that the SPICE model is valid for these devices. The tools needed for the extraction methods include a suitable scientific calculator (programmable, if possible) which is capable of performing statistical calculations, and an understanding of linear and nonlinear least-squares curve fitting methods.

For some parameters, more than one method of extraction may be given. To determine which method is *best* in providing a set of parameters yielding the most accurate simulation, it is necessary to examine the differences between actual device data and the results provided by the model equations when using these parameters. By defining these differences as *errors*, a single quantity can be calculated for each method that can be used as a basis of comparison. This quantity is called the *error function*  $E_2$  which is the sum of the squares of the magnitudes of the per unit or normalized errors between actual device data and the corresponding data generated by the model. This function is represented by the equation given below

$$E_2 = |\epsilon_1|^2 + |\epsilon_2|^2 + \dots + |\epsilon_n|^2 = \sum |\epsilon_i|^2 \quad (3.35)$$

where  $\epsilon_i$  is the normalized error of the  $i$ th data point and  $n$  is the number of data points [7]. For most modeling applications, the method which produces the smallest value of  $E_2$  is therefore judged the best method and the parameters extracted with this method provide the most accurate results

### Forward DC Characteristics (IS, RS, N)

There are three methods for the extraction of the parameters IS, RS, and N which model the large-signal dc behavior in the forward-bias region. The first method computes these parameters from three points taken from the forward-bias I-V curve and is appropriately called the *three-point I-V method*. The second method uses a fixed value of RS (which can be taken from the results of the three-point I-V method) and performs a linear regression data fit over the I-V curve to extract IS and N. The third method uses a fixed value of IS and performs a nonlinear data fit to extract N and RS. This method is useful if the reverse leakage current  $I_R$  is specified and is to be modeled by IS.

1. *Method 1 (Three-point I-V method).* To use this method, it is necessary to have a plot of the dc forward-bias I-V curve where the current axis is logarithmically scaled and the voltage axis is linearly scaled as shown in Figure 3.11. Estimated values for the parameters can be found from the steps outlined below.

- (i) Select three data points from the I-V curve shown as points 1, 2, and 3.
- (ii) Using the values of current and voltage corresponding to these points as indicated, calculate values for the parameters RS, N, and IS from the following equations

$$RS = \frac{(V_{F2} - V_{F1}) + (V_{F1} - V_{F3}) \cdot \left[ \frac{\ln \left( \frac{I_{D1}}{I_{D2}} \right)}{\ln \left( \frac{I_{D1}}{I_{D3}} \right)} \right]}{(I_{D2} - I_{D1}) + (I_{D1} - I_{D3}) \cdot \left[ \frac{\ln \left( \frac{I_{D1}}{I_{D2}} \right)}{\ln \left( \frac{I_{D1}}{I_{D3}} \right)} \right]} \quad (3.36)$$

$$N = \frac{(V_{F1} - V_{F2}) + RS \cdot (I_{D2} - I_{D1})}{V_t \cdot \ln \left( \frac{I_{D1}}{I_{D2}} \right)} \quad (3.37)$$

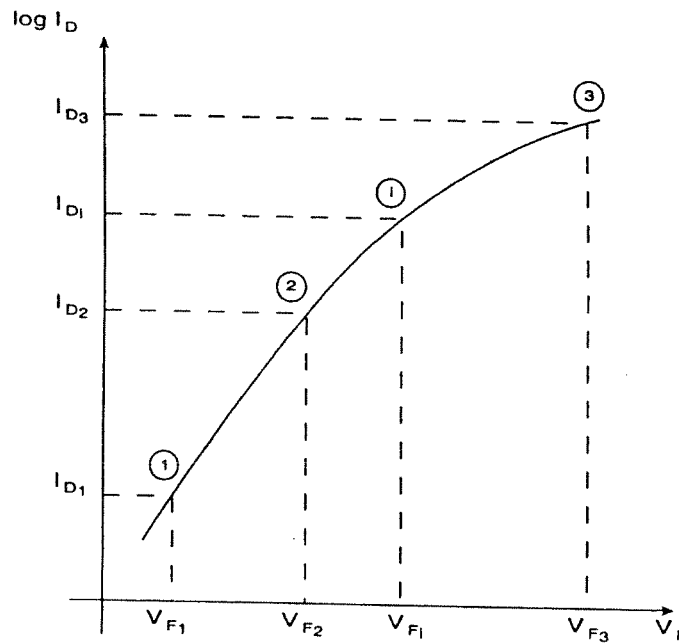


FIGURE 3.11 Forward-bias DC Data for the Three-point I-V Method.

$$IS = \frac{I_{Di}}{\exp\left(\frac{V_{Fi} - RS \cdot I_{Di}}{N \cdot V_t}\right) - 1} \quad (3.38)$$

2. *Method 2 (Linear regression with fixed RS).* With this method, a linear regression data fit is performed on the data covering the full range of the I-V curve to an equation of a straight line which represents the diode dc characteristics. This equation can be derived by combining Equations 3.1 and 3.3 to produce

$$I_{Di} = IS \cdot \left\{ \exp\left(\frac{V_{Fi} - RS \cdot I_{Di}}{N \cdot V_t}\right) - 1 \right\} \quad (3.39)$$

where  $I_{Di}$  and  $V_{Fi}$  represent the  $i$ th data point taken from  $n$  data points on the I-V curve (shown in Figure 3.11), and  $RS$  is a known value of the ohmic resistance parameter. Assuming that the exponential term is sufficiently large, this equation can be approximated by

$$I_{Di} \cong IS \cdot \exp\left(\frac{V_{Fi} - RS \cdot I_{Di}}{N \cdot V_t}\right) \quad (3.40)$$

Taking the natural logarithm of both sides yields

$$\ln(I_{Di}) = \ln(IS) + \frac{1}{N} \cdot \left( \frac{V_{Fi} - RS \cdot I_{Di}}{V_t} \right) \quad (3.41)$$

which is the equation of a straight line expressed as

$$y_i = b + m \cdot x_i \quad (3.42)$$

where

$$y_i = \ln(I_{Di}) \quad (3.43)$$

$$x_i = \left( \frac{V_{Fi} - RS \cdot I_{Di}}{V_t} \right) \quad (3.44)$$

$$b = \ln(IS) \quad (3.45)$$

and

$$m = \frac{1}{N} \quad (3.46)$$

The constants  $b$  and  $m$  are the y-axis intercept and slope, respectively, of the straight line represented by Equation 3.42. Values for these constants can be found by solving the matrix equation

$$\begin{bmatrix} n & \Sigma(x_i) \\ \Sigma(x_i) & \Sigma(x_i)^2 \end{bmatrix} \cdot \begin{bmatrix} b \\ m \end{bmatrix} = \begin{bmatrix} \Sigma(y_i) \\ \Sigma(x_i) \cdot (y_i) \end{bmatrix} \quad (3.47)$$

where the summations are taken over the  $n$  data points. The calculated values of  $b$  and  $m$  are then used to find  $IS$  and  $N$  from Equations 3.45 and 3.46 where

$$IS = \exp(b) \quad (3.48)$$



and

$$N = \frac{1}{m} \quad (3.49)$$

It is important to note that many scientific calculators have built-in statistical functions capable of performing linear regression calculations. For the type of equations used in this method, these functions can be used to extract the parameters IS and N directly. This, of course, eliminates the need to generate and solve Equation 3.47. The steps involved in this method are outlined below.

- (i) Select a value of RS which may be the value calculated from Equation 3.36 in Method 1.
  - (ii) Perform a linear regression data fit on  $n$  data points taken from the I–V curve to Equation 3.42 where the  $y_i$  and  $x_i$  data values are calculated from Equations 3.43 and 3.44. This data fit will give values for  $b$  and  $m$ .
  - (iii) Calculate the values of IS and N from Equations 3.48 and 3.49, respectively.
3. *Method 3 (Nonlinear curve fit with fixed IS).* The techniques used in this method are similar to those of Method 2 except that IS is held fixed, and RS and N are extracted. This method is particularly useful when IS must model a known value of the reverse leakage current. The equation for the curve fit is derived from Equation 3.39 where voltage is expressed as the dependent variable; that is

$$V_{Fi} = N \cdot V_i \ln \left( \frac{I_{Di}}{IS} + 1 \right) + RS \cdot I_{Di} \quad (3.50)$$

where  $I_{Di}$  and  $V_{Fi}$  again represent the  $i$ th data point taken from  $n$  data points on the I–V curve, and IS is a known value of the saturation current parameter. This equation may be expressed as a linear combination of two functions of the current in the form of

$$y_i = a_1 \cdot f_1(I_{Di}) + a_2 \cdot f_2(I_{Di}) \quad (3.51)$$

where

$$y_i = V_{Fi} \quad (3.52)$$

$$f_1(I_{Di}) = V_i \cdot \ln \left( \frac{I_{Di}}{IS} + 1 \right) \quad (3.53)$$

$$f_2(I_{Di}) = I_{Di} \quad (3.54)$$

$$a_1 = N \quad (3.55)$$

and

$$a_2 = RS \quad (3.56)$$

The constants  $a_1$  and  $a_2$  are found from the solution of a matrix equation similar in appearance to that of Equation 3.47 where

$$\begin{bmatrix} \sum [f_1(I_{Di})]^2 & \sum [f_1(I_{Di}) \cdot f_2(I_{Di})] \\ \sum [f_1(I_{Di}) \cdot f_2(I_{Di})] & \sum [f_2(I_{Di})]^2 \end{bmatrix} \cdot \begin{bmatrix} a_1 \\ a_2 \end{bmatrix} = \begin{bmatrix} \sum [y_i \cdot f_1(I_{Di})] \\ \sum [y_i \cdot f_2(I_{Di})] \end{bmatrix} \quad (3.57)$$

The summations for the elements of this matrix equation are again taken over the  $n$  data points. Values of  $a_1$  and  $a_2$  found from this equation are then used to calculate  $N$  and  $RS$  where

$$N = a_1 \quad (3.58)$$

and

$$RS = a_2 \quad (3.59)$$

The details explaining more on the techniques of this method may be found in [8]. The steps involved in this method are outlined below.

- (i) Select a value of  $IS$  which may be that of the reverse leakage current at a value of specified reverse-bias voltage.
- (ii) Generate the matrix Equation 3.57 where  $y_i$  and the functions  $f_1(I_{Di})$  and  $f_2(I_{Di})$  are calculated from Equations 3.52 through 3.54 for the  $n$  data points taken from the I-V curve.
- (iii) Solve this matrix equation for the constants  $a_1$  and  $a_2$ , and calculate the values of  $N$  and  $RS$  from Equations 3.58 and 3.59, respectively.

### Junction Capacitance Characteristics (CJO, VJ, M, FC)

There are two methods for the extraction of the parameters CJO, VJ, M and FC which model the behavior of the junction capacitance. The first method computes these parameters from three points taken from the reverse-bias C-V curve and is appropriately called the *three-point C-V method*. The second method uses a fixed value of VJ (which can be taken from the results of the three-point C-V method) and performs a linear regression data fit over the C-V curve to extract CJO and M. In both methods, the parameter FC is set to the default value of 0.5 since forward-bias capacitance information is rarely presented on most diode data sheets.

1. *Method 1 (Three-point C-V method)*. To use this method, it is necessary to have a plot of the reverse-bias junction capacitance curve ( $C_j$  versus  $V_R$ ) where each axis is logarithmically scaled as shown in Figure 3.12.
  - (i) Select a data point at the lower end of the C-V curve shown as point 1. The voltage at this point should be less than the typical ideal value of VJ (that is, 0.8 volt to 1.0 volt).
  - (ii) Select two data points at the upper end of the curve shown as points 2 and 3. The voltages at these points should be much greater than the typical ideal value of VJ.
  - (iii) Using the values of capacitance and voltage corresponding to these points as indicated, calculate values for the parameters M, VJ, CJO, and FC from the following equations

$$M = \frac{\ln\left(\frac{C_{j2}}{C_{j3}}\right)}{\ln\left(\frac{V_{R3}}{V_{R2}}\right)} \quad (3.60)$$

$$k_1 = \left(\frac{C_{j1}}{C_{j2}}\right)^{1/M} \quad (\text{a constant}) \quad (3.61)$$

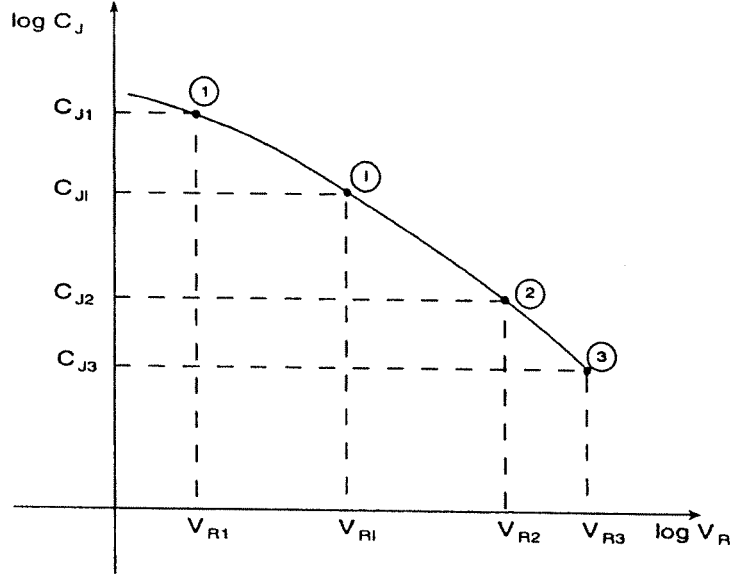


**FIGURE 3.12** Reverse-bias Junction Capacitance Data for the Three-point C-V Method.

$$VJ = \frac{k_1 \cdot V_{R1} - V_{R2}}{1 - k_1} \quad (3.62)$$

$$CJO = C_{J1} \cdot \left(1 + \frac{V_{R1}}{VJ}\right)^M \quad (3.63)$$

$$FC = 0.5 \quad (3.64)$$

2. *Method 2 (Linear regression with fixed VJ).* With this method, a linear regression data fit is performed on the data covering the full range of the reverse-bias C-V curve to an equation of a straight line representing the capacitance characteristics in this region. For reverse-bias voltages, Equation 3.10 can be expressed as

$$C_{ji} = CJO \cdot \left(1 + \frac{V_{Ri}}{VJ}\right)^{-M} \quad (3.65)$$

where  $C_{ji}$  and  $V_{Ri}$  represent the  $i$ th data point taken from  $n$  data points on the C-V curve (shown in Figure 3.12), and  $VJ$  is a known value of the contact potential parameter. Taking the natural logarithm of both sides yields

$$\ln(C_{ji}) = \ln(CJO) - M \cdot \ln\left(1 + \frac{V_{Ri}}{VJ}\right) \quad (3.66)$$

which is the equation of a straight line expressed as

$$Y_i = b + m \cdot x_i \quad (3.67)$$

where

$$y_i = \ln(C_{ji}) \quad (3.68)$$

$$x_i = \ln \left( 1 + \frac{V_{Ri}}{VJ} \right) \quad (3.69)$$

$$b = \ln(CJO) \quad (3.70)$$

and

$$m = -M \quad (3.71)$$

The constants  $b$  and  $m$  are the y-axis intercept and slope, respectively, of the straight line represented by Equation 3.67. Values for these constants can be found by solving a matrix equation similar to that of equation 3.47 or by using the linear regression function on the calculator. The parameters CJO and M are then calculated from

$$CJO = \exp(b) \quad (3.72)$$

and

$$M = -m \quad (3.73)$$

The steps for this method are outlined below.

- (i) Select a value of VJ which may be the value calculated from Equation 3.62 in Method 1.
- (ii) Perform a linear regression data fit on  $n$  data points taken from the C-V curve to Equation 3.67 where the  $y_i$  and  $x_i$  data values are calculated from Equations 3.68 and 3.69. This data fit will give values for  $b$  and  $m$ .
- (iii) Calculate the values of CJO and M from Equations 3.72 and 3.73, respectively, and the value of FC from Equation 3.64.

### Reverse Recovery Time Characteristics (TT)

For the extraction of the forward transit time parameter TT, the results of reverse recovery time ( $t_{rr}$ ) measurements derived by Leinfelder are employed [9]. The common JEDEC test circuit for measuring  $t_{rr}$  is shown in Figure 3.13 while the idealized time-domain waveform of the diode current resulting from this circuit is shown in Figure 3.14. The reverse recovery time  $t_{rr}$  is commonly measured between the time that the current (previously forward biased at  $I_F$ ) passes through zero going negatively and the time that the reverse current recovers to a value which is less than 10% of the peak reverse current  $I_{RM}$  [10]. From Figure 3.14,  $t_{rr}$  is shown to consist of  $t_{\phi}$  which is the time for the diffusion charge supporting the reverse current to reduce to zero, and  $t_b$  which is the time for the depletion charge supporting the forward voltage to also reduce to zero. At the end of  $t_{rr}$  the diode is turned off and cannot sustain the reverse current. The total charge depleted from the diode during the reverse recovery time is called the *reverse recovery charge*  $Q_{rr}$  which is the sum of the charges  $Q_a$  and  $Q_b$  represented by the areas under the waveform during times  $t_a$  and  $t_b$ , respectively. By assuming that  $Q_{rr}$  is dominated by the charge  $Q_a$  so that the reverse recovery time  $t_{rr}$  is approximately equal to  $t_{\phi}$ , the following equations can be generated from the information shown on Figure 3.14. For the current fall-time  $t_f$ :

$$t_f = \frac{I_F}{\left( \frac{di}{dt} \right)} \quad (3.74)$$

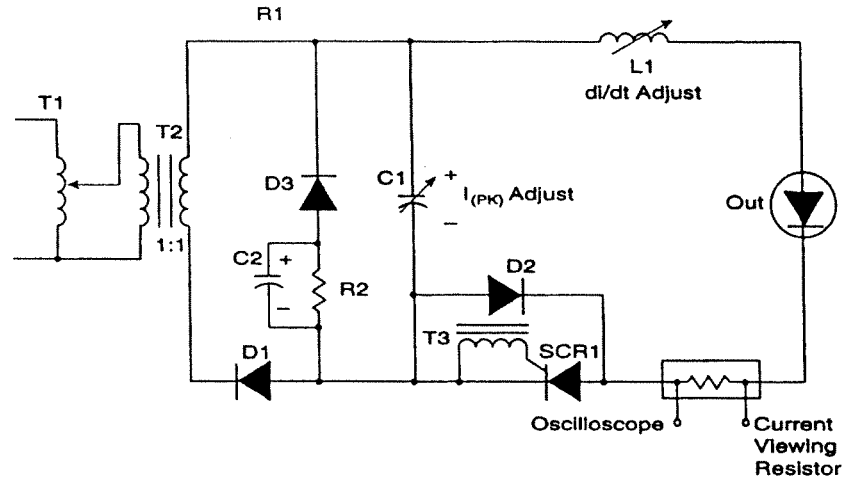


FIGURE 3.13 JEDEC Reverse Recovery Time Test Circuit.

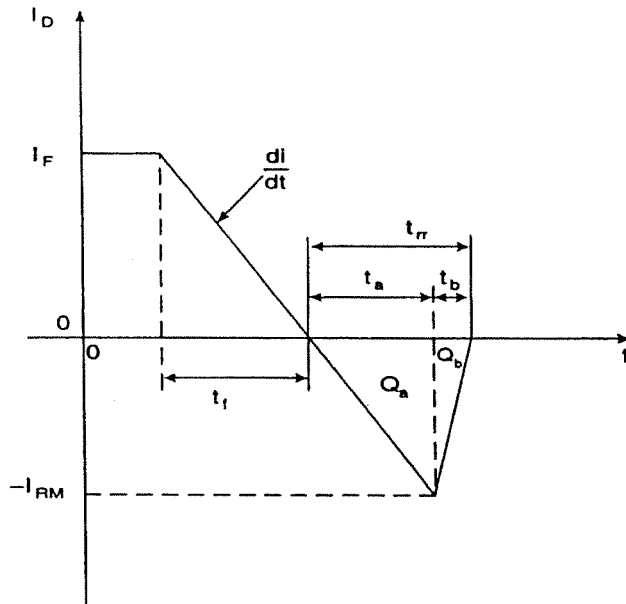


FIGURE 3.14 Idealized Time-domain Waveform for the Diode Current from the Test Circuit of Figure 3.13.

where  $I_F$  is the forward-bias diode current in amps and  $di/dt$  is the slew-rate in amp/second of the current set by the circuit. The expression for  $t_{rr}$  is:

$$t_{rr} \equiv t_a = \frac{I_{RM}}{\left(\frac{di}{dt}\right)} \quad (3.75)$$

where  $I_{RM}$  is the peak reverse current. Assuming that the reverse recovery charge  $Q_{rr}$

is approximately equal to the charge  $Q_a$ , the area under the triangle corresponding to this charge is computed from

$$Q_{rr} \cong Q_a = \frac{t_a \cdot I_{RM}}{2} = \frac{t_a^2}{2} \cdot \left(\frac{di}{dt}\right) = \frac{t_{rr}^2}{2} \cdot \left(\frac{di}{dt}\right) \quad (3.76)$$

From Leinfelder's work, an expression for  $Q_{rr}$  was derived from curve-fitting methods and was found to be accurate for simulating  $t_{rr}$ . This expression is given as

$$Q_{rr} = I_F \cdot TT \cdot \exp\left(-\sqrt{\frac{t_f}{TT}}\right) = I_F \cdot TT \cdot \exp\left(-\sqrt{\frac{I_F}{TT \cdot \left(\frac{di}{dt}\right)}}\right) \quad (3.77)$$

where TT is, of course, the forward transit time parameter. By setting Equations 3.76 and 3.77 equal to each other, a single expression involving TT is derived

$$\frac{t_{rr}^2}{2} \cdot \left(\frac{di}{dt}\right) = I_F \cdot TT \cdot \exp\left(-\sqrt{\frac{I_F}{TT \cdot \left(\frac{di}{dt}\right)}}\right) \quad (3.78)$$

Thus, by knowing  $t_{rr}$ ,  $I_F$ , and the current slew-rate  $di/dt$ , Equation 3.78 can be solved iteratively to find TT. Numerical algorithms such as *Newton's method* can be used on this equation which is easily implemented on a programmable calculator [7].

The steps for extracting the parameter TT are outlined below.

- (i) From the device data sheet, determine values for the reverse recovery time  $t_{rr}$ , the forward-bias diode current  $I_F$ , and the slew-rate of the current waveform  $di/dt$ .
- (ii) Generate a function of the forward transit time TT where:

$$f(TT) = \frac{t_{rr}^2}{2} \cdot \left(\frac{di}{dt}\right) - I_F \cdot TT \cdot \exp\left(-\sqrt{\frac{I_F}{TT \cdot \left(\frac{di}{dt}\right)}}\right) \quad (3.79)$$

- (iii) Use Newton's method to solve Equation 3.79 for the value of TT that will set  $f(TT)$  to zero.

### Temperature Characteristics (EG, XTI)

There are three methods for the extraction of the parameters EG and XTI. In each of these methods, only one temperature-dependent expression is used where EG is selected and XTI is calculated. The first method uses the small-scale expression for the voltage temperature coefficient TCV found from the derivative of the voltage  $V_F$  with respect to temperature. The second method uses the large-scale expression for the TCV which is derived from the change of the diode forward voltage over large temperature changes. The third method uses the expression for the temperature-

dependent saturation current  $I_S$  given in Equation 3.21 to model the temperature behavior of the reverse leakage current  $I_R$ . In all of the equations used in these methods, temperature values must be converted to degrees Kelvin ( $^{\circ}\text{K}$ ).

1. *Method 1 (Small-scale TCV method)*. From Equations 3.1 and 3.3, the expression for the diode forward voltage as a function of temperature is derived as:

$$V_f(T) = N \cdot V_i(T) \cdot \ln\left(\frac{I_D}{I_S(T)} + 1\right) + RS \cdot I_D \quad (3.80)$$

Using the temperature-dependent expression for the saturation current  $I_S$  given in Equation 3.21, the small-scale or derivative form of the voltage temperature coefficient TCV is derived and shown below

$$TCV = \left. \frac{dV_f(T)}{dT} \right|_{I_D, T} = \frac{\left\{ N \cdot V_i(T) \cdot \ln\left(\frac{I_D}{I_S(T)} + 1\right) - (EG + XTI \cdot V_i(T)) \right\}}{T} \quad (3.81)$$

where  $I_D$  is the forward current and  $T$  is the temperature at which the TCV is measured, usually  $27^{\circ}\text{C}$ . This equation is now used to find  $EG$  and  $XTI$  with the steps outlined below.

- (i) From the data sheet, determine the value of the TCV, and the values of the forward current  $I_D$  and the temperature  $T$  corresponding to the TCV.
- (ii) Select a suitable value for the energy gap  $EG$  which should correspond to the type of material used to process the diode (for example, 1.11 eV for silicon).
- (iii) Solve for the value of the parameter  $XTI$  from Equation 3.81 where

$$XTI = \left( \frac{1}{V_i(T)} \right) \cdot \left\{ N \cdot V_i(T) \cdot \ln\left(\frac{I_D}{I_S(T)} + 1\right) - (EG + T \cdot TCV) \right\} \quad (3.82)$$

2. *Method 2 (Large-scale TCV method)*. Again from Equation 3.80, the large-scale form of the voltage temperature coefficient is derived and shown below

$$TCV = \frac{\Delta V_f(T)}{\Delta T} = \left. \frac{V_f(T_1) - V_f(T_o)}{T_1 - T_o} \right|_{I_D}$$

$$= \left( \frac{1}{T_o} \right) \cdot \left\{ N \cdot V_i(T_o) \cdot \ln\left(\frac{I_D}{I_S(T_o)}\right) - [EG + XTI \cdot V_i(T_o) \cdot \left( \frac{T_1 \cdot \ln\left(\frac{T_1}{T_o}\right)}{T_1 - T_o} \right)] \right\} \quad (3.83)$$

where  $T_1$  is a temperature read from the data sheet,  $T_o$  is room temperature of  $27^{\circ}\text{C}$ ,  $V_f(T_1)$  and  $V_f(T_o)$  are the diode voltages at these temperatures, and  $I_D$  is the forward current, all of which are shown on the typical I-V curve of Figure 3.15. This equation and data are used to find  $EG$  and  $XTI$  with the steps outlined below.

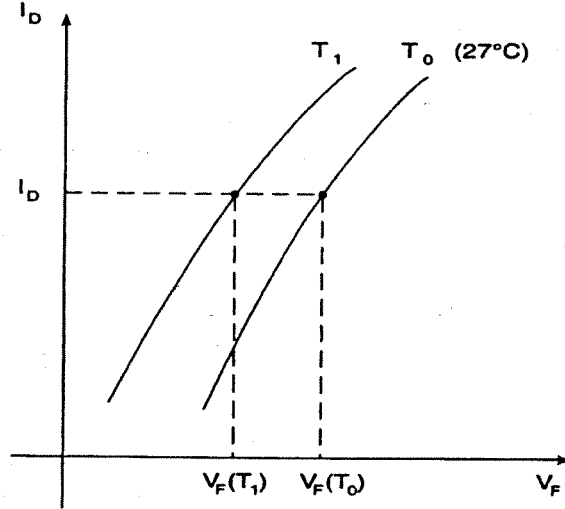


FIGURE 3.15 Typical Forward-bias Diode Voltage Temperature Characteristics.

- (i) From the data sheet I-V curve plotted for at least two temperatures, calculate the large-scale TCV at the current  $I_D$  from the expression

$$TCV = \left. \frac{V_F(T_1) - V_F(T_0)}{T_1 - T_0} \right|_{I_D} \quad (3.84)$$

- (ii) Select a suitable value for the energy gap EG which should correspond to the type of material used to process the diode (for example, 1.11 eV for silicon).  
 (iii) Solve for the value of the parameter XTI from Equation 3.83 where

$$XTI = \frac{\left\{ N \cdot V_T(T_0) \cdot \ln \left( \frac{I_D}{IS(T_0)} \right) - (EG + T_0 \cdot TCV) \right\}}{V_T(T_0) \cdot \left( \frac{T_1 \cdot \ln \left( \frac{T_1}{T_0} \right)}{T_1 - T_0} \right)} \quad (3.85)$$

3. *Method 3 (Reverse leakage current method).* Assuming that the temperature behavior of the diode reverse leakage current  $I_R$  can be modeled by that of the saturation current parameter IS, Equation 3.21 can be used directly to extract the parameters EG and XTI. From this equation, the temperature-dependence of  $I_R$  can be written as

$$I_R(T_1) = I_R(T_0) \cdot \left( \frac{T_1}{T_0} \right)^{XTI/N} \cdot \exp \left\{ \left( \frac{q \cdot EG}{N \cdot k} \right) \cdot \left( \frac{1}{T_0} - \frac{1}{T_1} \right) \right\} \quad (3.86)$$

where  $T_1$  is a temperature read from the data sheet,  $T_0$  is room temperature of 27°C, and  $I_R(T_1)$  and  $I_R(T_0)$  are the leakage currents at these temperatures, all of



which are shown on the typical  $I_R$  versus temperature curve of Figure 3.16. Equation 3.86 and this data are used to find EG and XTI with the steps outlined below.

- (i) From the data sheet reverse leakage current versus temperature ( $I_R$  versus  $T$ ) curve, select values of the leakage current at the temperatures  $T_o$  ( $27^\circ\text{C}$ ) and  $T_1$ ; that is,  $I_R(T_o)$  and  $I_R(T_1)$ .
- (ii) Select a suitable value for the energy gap EG which should correspond to the type of material used to process the diode (for example, 1.11 eV for silicon).
- (iii) solve for the value of the parameter XTI from Equation 3.86 where

$$XTI = \frac{\left\{ N \cdot \ln \left( \frac{I_R(T_1)}{I_R(T_o)} \right) - \frac{q \cdot EG}{k} \cdot \left( \frac{1}{T_o} - \frac{1}{T_1} \right) \right\}}{\ln \left( \frac{T_1}{T_o} \right)} \quad (3.87)$$

### Reverse Breakdown Characteristics (BV, IBV)

The steps for extracting the parameters BV and IBV are outlined below.

- (i) From the device data sheet, determine the value of the maximum dc blocking voltage  $V_R(\text{max})$ .
- (ii) Multiply this voltage by a constant  $k_{BV}$  having a value ranging from about 1.3 to 2.0. This will account for the amount of manufacturers guard-band placed on the breakdown voltage in order to insure the maximum voltage rating. This operation produces the value for the breakdown voltage parameter BV where

$$BV = k_{BV} \cdot V_R(\text{max}) \quad (3.88)$$

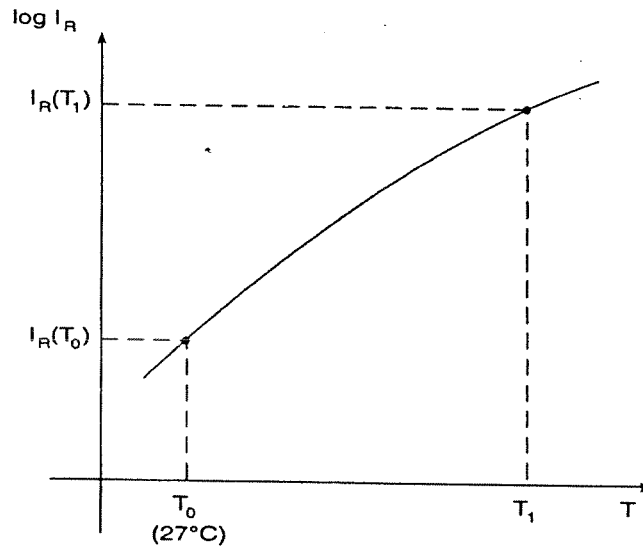


FIGURE 3.16 Typical Reverse Leakage Current Temperature Characteristics.

(iii) Calculate the value  $IBV$  from

$$IBV = (1.1) \cdot \frac{IS(T_{\max}) \cdot BV}{V_t(T_{\max})} \quad (3.89)$$

where the 1.1 multiplier insures the inequality in Equation 3.8 and  $T_{\max}$  is the maximum simulation temperature.

## Example Parameter Extractions for the MURH840CT Diode

As an example of the methods presented in the last section, the SPICE model parameters will be extracted for the Motorola MURH840CT rectifier with the aid of a programmable scientific calculator. Pertinent characteristic curves taken from the device data sheet will be used to provide the necessary data for the extraction. In the processes that are to follow, particular attention will be placed not only on these curves but also on certain tabular information regarding maximum ratings and electrical characteristics. It is important that this data is included in the determination of the parameters since the model must simulate as closely as possible all characteristics of the diode.

It is industry practice to use 25°C as room temperature. For the extraction process, the SPICE default of 27°C will be used instead and it will be assumed that the 2°C difference will not produce any significant errors. At 27°C, the value for the thermal voltage  $V_t$  which is used in several of the extraction methods is calculated from Equation 3.7 where

$$V_t = 25.85562 \text{ mV} \quad (3.90)$$

For consistency, the order of parameter extraction will follow that of the last section which begins with the forward dc characteristics.

### Forward DC Characteristics ( $IS$ , $RS$ , $N$ )

The forward-bias I–V curve for the MURH840CT rectifier is shown in Figure 3.17. Data from this curve will be used in each of the three methods for extracting the parameters  $IS$ ,  $RS$ , and  $N$ .

1. *Method 1 (Three-point I–V method).* As shown in Figure 3.17, three points are selected on the I–V curve at 25°C as points 1 through 3. The current and voltage values corresponding to these points are listed in Table 3.3. From Equations 3.36 through 3.38, the following parameters are computed from this data for 27°C:

$$RS = 40.20590 \text{ m}\Omega \quad (3.91)$$

$$N = 2.854546 \quad (3.92)$$

and

$$IS = 3.255398 \text{ }\mu\text{A} \quad (3.93)$$

2. *Method 2 (Linear regression with fixed  $RS$ ).* From Figure 3.17, the I–V data given in Table 3.4 is obtained. These 10 I–V data points are transformed into  $x$ - $y$  data points with Equations 3.43 and 3.44 where

$$y_i = \ln(I_{Di}) \quad (3.94)$$

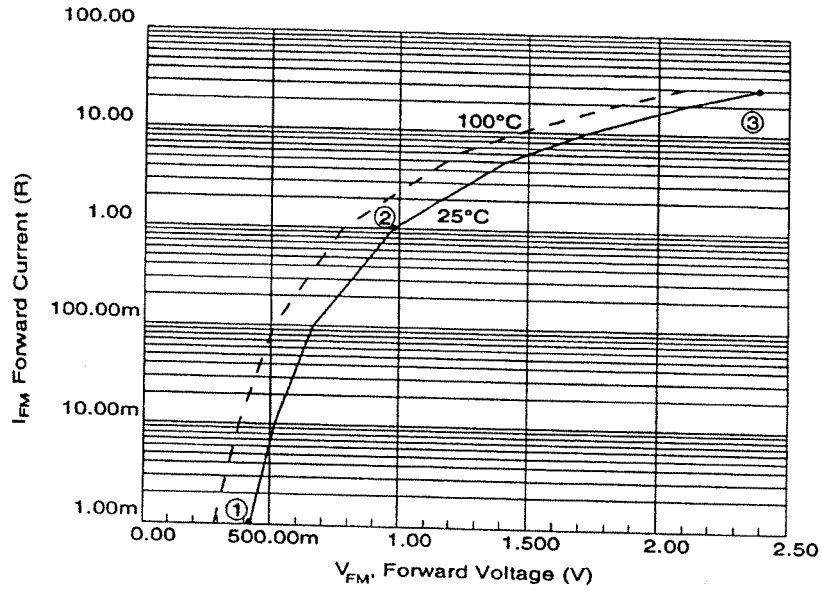


FIGURE 3.17 MURH840CT Forward-bias DC Data for the Three-point I-V Method.

TABLE 3.3 Data for the Three-Point I-V Method

Point	Diode forward current ( $I_D$ ) (A)	Diode forward voltage ( $V_F$ ) (V)
1	1.0m	0.423
2	1.0	0.973
3	30.0	2.390

TABLE 3.4 Forward Current Versus Forward Voltage for the MURH840CT

Diode forward current ( $I_D$ ) (A)	Diode forward voltage ( $V_F$ ) (V)
1.0m	0.423
10.0m	0.512
100.0m	0.663
1.0	0.973
5.0	1.408
10.0	1.706
15.0	1.925
20.0	2.104
25.0	2.256
30.0	2.390

and

$$x_i = \left( \frac{V_{Fi} - RS \cdot I_{Di}}{V_i} \right) \quad (3.95)$$

for  $i = 1$  to 10. The value of  $RS$  used in Equation 3.95 is that found from the results of Method 1 given in Equation 3.91. For a linear regression data fit using

this transformed data, the matrix equation below is generated from Equation 3.47

$$\begin{bmatrix} 10 & 390.3876 \\ 390.3876 & 16911.02 \end{bmatrix} \cdot \begin{bmatrix} b \\ m \end{bmatrix} = \begin{bmatrix} 2.420368 \\ 528.9597 \end{bmatrix} \quad (3.96)$$

This equation is solved for  $b$  and  $m$  where

$$b = -9.909661 \quad (3.97)$$

and

$$m = 0.2600451 \quad (3.98)$$

From Equations 3.48 and 3.49, values for the parameters  $IS$  and  $N$  are calculated, and presented with  $RS$  where

$$IS = \exp(b) = 49.69228 \mu A \quad (3.99)$$

$$N = \frac{1}{m} = 3.84554 \quad (3.100)$$

and

$$RS = 40.20590 \text{ m}\Omega \quad (3.101)$$

3. *Method 3 (Nonlinear curve fit with fixed  $IS$ )*. The maximum instantaneous reverse current ( $I_R$ ) at 25°C is specified on the data sheet as 10  $\mu A$ . Since this current is modeled by  $IS$ , it is necessary to keep its value less than 10  $\mu A$  in order to satisfy the maximum  $I_R$  specification. Thus, for this method,  $IS$  is set to 3.0  $\mu A$  which is close to the value at 25°C and 400 volts shown in the plot of reverse current versus reverse voltage of Figure 3.22. From Table 3.4, the 10 I-V data points are transformed into  $y$  data points with Equation 3.52, and the two current functions with Equations 3.53 and 3.54 where

$$Y_i = V_{Fi} \quad (3.102)$$

$$f_1(I_{Di}) = V_i \cdot \ln\left(\frac{I_{Di}}{IS} + 1\right) \quad (3.103)$$

and

$$f_2(I_{Di}) = I_{Di} \quad (3.104)$$

for  $i = 1$  to 10. The value of  $IS$  used in equation (103) is 3.0  $\mu A$ . For a nonlinear curve fit using this transformed data, the matrix equation below is generated from Equation 3.57

$$\begin{bmatrix} 1.202756 & 43.00399 \\ 43.00399 & 2276.01 \end{bmatrix} \cdot \begin{bmatrix} a_1 \\ a_2 \end{bmatrix} = \begin{bmatrix} 5.401513 \\ 224.1998 \end{bmatrix} \quad (3.105)$$

This equation is solved for  $a_1$  and  $a_2$  where

$$a_1 = 2.986477 \quad (3.106)$$

and

$$a_2 = 42.07777 \text{ m} \quad (3.107)$$

From Equations 3.58 and 3.59, values for the parameters  $N$  and  $RS$  are calculated, and presented with  $IS$  where

$$N = a_1 = 2.986477 \quad (3.108)$$

$$RS = a_2 = 42.07777 \text{ m}\Omega \quad (3.109)$$

and

$$IS = 3.0 \mu\text{A} \quad (3.110)$$

To determine which of these three sets of extracted parameters best simulates this example device, the diode forward voltage is calculated from the SPICE model and compared to the data sheet value at the same current. These calculations are performed for each set of the extracted parameters and listed in Table 3.5 where  $V_{FC}$  is the voltage calculated from

$$V_{FC} = N \cdot V_t \cdot \ln\left(\frac{I_D}{IS} + 1\right) + RS \cdot I_D \quad (3.111)$$

and  $\epsilon$  is the error in percent between the data sheet voltage  $V_F$  and  $V_{FC}$  calculated as

$$\epsilon = \frac{V_{FC} - V_F}{V_F} \cdot 100\% \quad (3.112)$$

At the bottom of this table are the error functions ( $E_2$ ) calculated from the errors generated by the results of each method in accordance with Equation 3.35. From an examination of these values, it is clear that the parameters extracted with Method 1 produce the lowest value for  $E_2$ . However, the forward voltage errors for currents beyond 1.0 A (where the device is most likely to be used) are significantly larger than those produced by the parameters extracted with the other two methods. The parameters extracted by Method 2 yield lower errors in this range even though it has a larger error function. However, the value of  $IS$  extracted by this method is too large to satisfy the data sheet specification for maximum  $I_R$ . The parameters extracted by Method 3 produce the largest error function of the three while having errors above

**TABLE 3.5** SPICE Diode Voltages and Percent Error for All Three Methods

MURH840CT Data Sheet Values		Method 1		Method 2		Method 3	
		IS = 3.255398 $\mu$ A RS = 40.20590m N = 2.854546		IS = 49.69228 $\mu$ A RS = 40.20590m N = 3.845540		IS = 3.0 $\mu$ A RS = 42.07777m N = 2.986477	
$I_D$ (A)	$V_F$ (V)	$V_{FC}$ (V)	$\epsilon$ (%)	$V_{FC}$ (V)	$\epsilon$ (%)	$V_{FC}$ (V)	$\epsilon$ (%)
1.0m	0.423	0.4230000	0.0000	0.3033381	-28.2889	0.4488392	6.1086
10.0m	0.512	0.5930908	15.8380	0.5283141	3.1864	0.6268089	22.4236
100.0m	0.663	0.7666325	15.6308	0.7604325	14.6957	0.8083743	21.9267
1.0	0.973	0.9727604	-0.0246	1.0255167	5.3974	1.0240414	5.2458
5.0	1.408	1.2523701	-11.0533	1.3463608	-4.3778	1.3166286	-6.4894
10.0	1.706	1.5045580	-11.8078	1.6163086	-5.2574	1.5805403	-7.3540
15.0	1.925	1.7355133	-9.8435	1.8576529	-3.4986	1.8222380	-5.3383
20.0	2.104	1.9577755	-6.9498	2.0872862	-0.7944	2.0548409	-2.3365
25.0	2.256	2.1752744	-3.5783	2.3105025	2.4159	2.2824602	1.1729
30.0	2.390	2.3897603	-0.0100	2.5296600	5.8435	2.5069275	4.8924
		$E_2 = 0.0914765$		$E_2 = 0.1155167$		$E_2 = 0.1203895$	

1.0 A comparable to those of Method 2. The value of  $I_S$  used in this method does, however, meet the maximum  $I_R$  specification. Plots of the dc characteristics resulting from each of the three methods are shown in Figures 3.18(a) through 3.18(c). Both data sheet and calculated voltages are plotted versus current to illustrate the closeness of data fit.

At this point in the extraction process, a decision must be made as to which of the three parameter sets should be used to most accurately model the device in a practical and realistic manner. If the maximum  $I_R$  specification (at both 25°C and 150°C) can be waived, then the parameters extracted with Method 2 should be used. If this waiver cannot be exercised, which is often the case, then the parameters from Method 3 should be used in spite of the inaccuracy of the data fit for currents below 1.0 A. For this example, the maximum  $I_R$  specification will be observed and the parameters extracted by Method 3 will be used.

### Junction Capacitance Characteristics (CJO, VJ, M, FC)

The reverse-bias C–V curve for the MURH840CT is shown in Figure 3.19. Data from this curve will be used in each of the two methods for extracting the parameters CJO, VJ, M and FC.

1. *Method 1 (Three-point C–V method).* From Figure 3.19, a point is selected at the lower voltage end of the C–V curve as point 1. Points 2 and 3 are selected at the upper voltage end as indicated. The capacitance and reverse voltage values corresponding to these points are shown in Table 3.6.

From Equations 3.60 through 3.64, the following junction capacitance parameters are computed from this data:

$$M = 0.4012080 \quad (3.113)$$

$$VJ = 0.2159243 \text{ V} \quad (3.114)$$

$$CJO = 152.7494 \text{ pF} \quad (3.115)$$

and

$$FC = 0.5 \quad (3.116)$$

2. *Method 2 (Linear regression with fixed VJ).* From Figure 3.19, the C–V data presented in Table 3.7 is obtained. These 11 C–V data points are transformed into  $x$ - $y$  data points with Equations 3.68 and 3.69 where

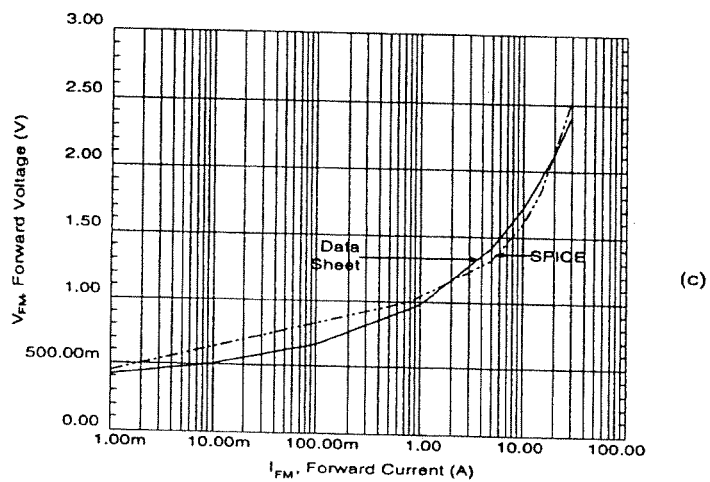
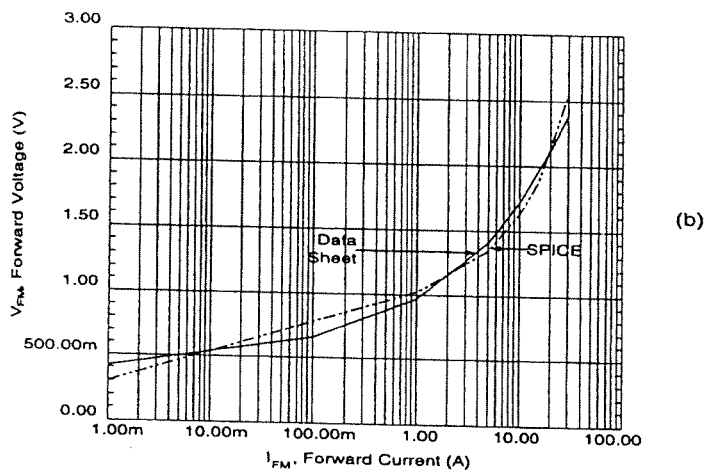
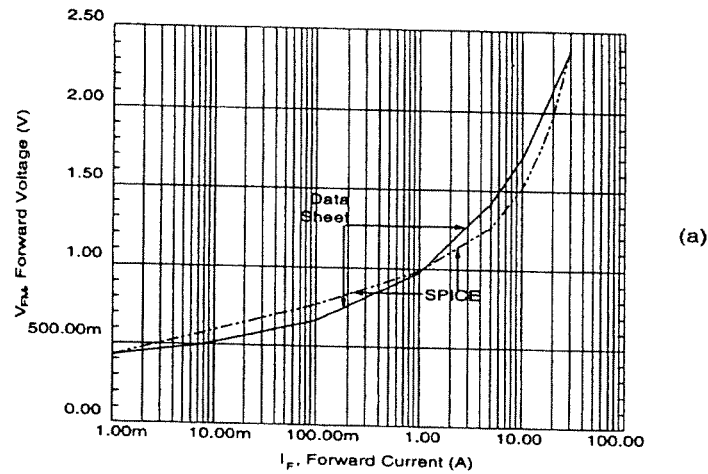
$$y_i = \ln(C_{ji}) \quad (3.117)$$

and

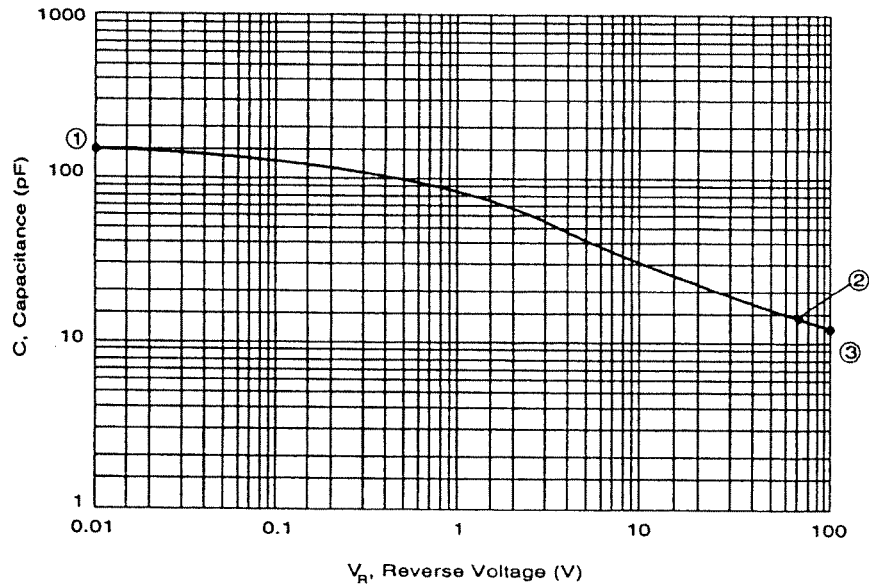
$$x_i = \ln\left(1 + \frac{V_{Ri}}{VJ}\right) \quad (3.118)$$

TABLE 3.6 Data for the Three-Point C–V Method

Point	Diode reverse voltage ( $V_R$ ) (V)	Diode junction capacitance ( $C_j$ ) (pF)
1	0.01	150.0
2	70.0	15.0
3	100.0	13.0



**FIGURE 3.18** (a) MURH840CT DC Characteristics from Method 1; (b) MURH840CT DC Characteristics from Method 2; (c) MURH840CT DC Characteristics from Method 3.



**FIGURE 3.19** MURH840CT Reverse-bias Junction Capacitance Data for the Three-point C-V Method.

**TABLE 3.7** Junction Capacitance Versus Reverse Voltage for the MURH840CT

Diode reverse voltage ( $V_R$ ) (V)	Diode junction capacitance ( $C_j$ ) (pF)
0.01	150.0
0.10	130.0
0.40	100.0
0.70	90.0
1.00	80.0
2.50	60.0
5.50	40.0
10.00	30.0
30.00	20.0
70.00	15.0
100.00	13.0

for  $i = 1$  to 11. The value of  $VJ$  used in Equation 3.118 is that found from the results of Method 1 given in Equation 3.114. For a linear regression data fit using this transformed data, the matrix equation below is generated from Equation 3.47:

$$\begin{bmatrix} 11 & 31.17795 \\ 31.17795 & 133.9153 \end{bmatrix} \cdot \begin{bmatrix} b \\ m \end{bmatrix} = \begin{bmatrix} -261.1229 \\ -758.7108 \end{bmatrix} \quad (3.119)$$

This equation is solved for  $b$  and  $m$  where

$$b = -22.58128 \quad (3.120)$$



and

$$m = -0.4082637 \quad (3.121)$$

From Equations 3.72 and 3.73, values for the parameters CJO and M are calculated, and presented with VJ and FC where

$$CJO = \exp(b) = 155.9821 \text{ pF} \quad (3.122)$$

$$M = -m = 0.4082637 \quad (3.123)$$

$$VJ = 0.2159243 \text{ V} \quad (3.124)$$

and

$$FC = 0.5 \quad (3.125)$$

To determine which of these two sets of extracted parameters best simulates this example device, the diode junction capacitance is calculated from the SPICE model and compared to the data sheet value at the same voltage. These calculations are performed for each set of parameters and listed in Table 3.8 where  $C_{jC}$  is the calculated capacitance

$$C_{jC} = CJO \cdot \left(1 + \frac{V_R}{VJ}\right)^{-M} \quad (3.126)$$

and  $\epsilon$  is the error in percent between the data sheet capacitance  $C_j$  and  $C_{jC}$  calculated as

$$\epsilon = \frac{C_{jC} - C_j}{C_j} \cdot 100\% \quad (3.127)$$

At the bottom of this table are the error functions ( $E_2$ ) calculated from the errors generated by the results of each method. From an examination of these values, it is clear that the parameters extracted with Method 2 produce the most accurate data fit to the actual device. Therefore, for this example, the parameters extracted by Method 2 will

**TABLE 3.8** SPICE Diode Junction Capacitances and Percent Error for Both Methods

MURH840CT Data Sheet Values		Method 1 CJO = 152.7494pF VJ = 0.2159243V M = 0.4012080 FC = 0.5		Method 2 CJO = 155.9821pF VJ = 0.2159243V M = 0.4082637 FC = 0.5	
		$C_{jC}$ (F)	$\epsilon$ (%)	$C_{jC}$ (F)	$\epsilon$ (%)
$V_R$ (V)	$C_j$ (F)				
10.0m	150.0p	150.0000p	0.0000	153.1256p	2.0837
100.0m	130.0p	131.1195p	0.8611	133.5354p	2.7195
400.0m	100.0p	100.3089p	0.3088	101.6770p	1.6769
700.0m	90.0p	85.5457p	-4.9492	86.4700p	-3.9222
1.0	80.0p	76.3538p	-4.5577	77.0247p	-3.7191
2.5	60.0p	55.3101p	-7.8164	55.4806p	-7.5323
5.5	40.0p	41.0343p	2.5857	40.9452p	2.3631
10.0	30.0p	32.5062p	8.3539	32.3030p	7.6767
30.0	20.0p	21.0384p	5.1922	20.7476p	3.7379
70.0	15.0p	15.0000p	0.0000	14.7049p	-1.9674
100.0	13.0p	13.0048p	0.0370	12.7170p	-2.1769
$E_2 = 0.021063 \quad E_2 = 0.018759$					

be used. Plots of the junction capacitance characteristics resulting from both methods are shown in Figures 3.20(a) and 3.20(b). Both data sheet and calculated capacitance are plotted versus reverse voltage to illustrate the closeness of data fit.

### Reverse Recovery Time Characteristics (TT)

The typical value for the reverse recovery time  $t_{rr}$  for the MURH840CT is 24.6 ns. This value is specified at a forward-bias current ( $I_F$ ) of 1.0 A and a current slew-rate

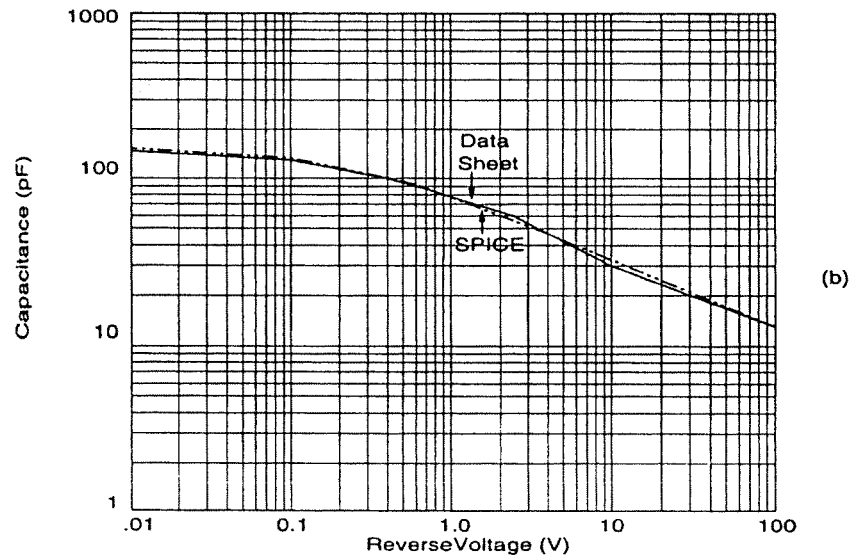
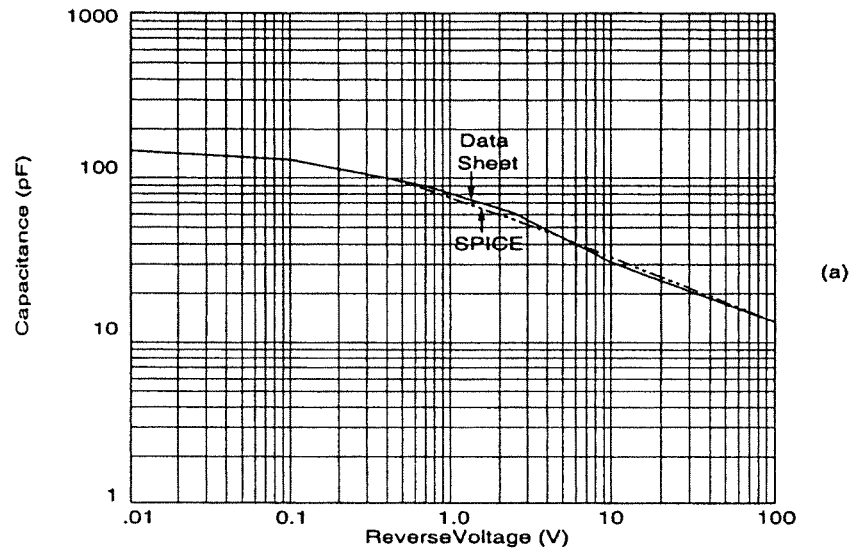


**FIGURE 3.20** (a) MURH840CT Junction Capacitance Characteristics from Method 1; (b) MURH840CT Junction Capacitance Characteristics from Method 2.

( $di/dt$ ) of 50 A/ $\mu$ s. The function equation for the forward transit time parameter TT generated from Equation 3.79 is shown below

$$f(TT) = 15.129 \cdot 10^{-9} - TT \cdot \exp\left(-\sqrt{\frac{20 \cdot 10^{-9}}{TT}}\right) = 0 \quad (3.128)$$

From Newton's method, the value of TT that satisfies this equation is found to be

$$TT = 32.96688 \text{ nseconds} \quad (3.129)$$

### Temperature Characteristics (EG, XTI)

The temperature characteristics of the MURH840CT are illustrated in Figures 3.21 and 3.22. Even though only three temperature points are given on these two plots, there is sufficient data available to allow the parameters EG and XTI to be extracted with Methods 2 and 3. Since information about the small-scale voltage temperature coefficient is not known, Method 1 will not be used.

1. *Method 2 (Large-scale TCV method).* The large-scale TCV is obtained from the forward-bias I-V curve of Figure 3.21. At a forward current ( $I_D$ ) of 1.0 A, the diode voltages at 25°C ( $T_0$ ) and 100°C ( $T_1$ ) are read as 0.973 V ( $V_F(T_0)$ ) and 0.776 V ( $V_F(T_1)$ ), respectively. The value of the large-scale TCV is calculated from Equation 3.84 where

$$TCV = -2.62667 \text{ mV/}^\circ\text{C} \quad (3.130)$$

Selecting the value for the energy gap parameter EG as 1.11 eV which is typical for silicon, the value for the parameter XTI is computed from equation (85) as

$$XTI = 23.702105 \quad (3.131)$$

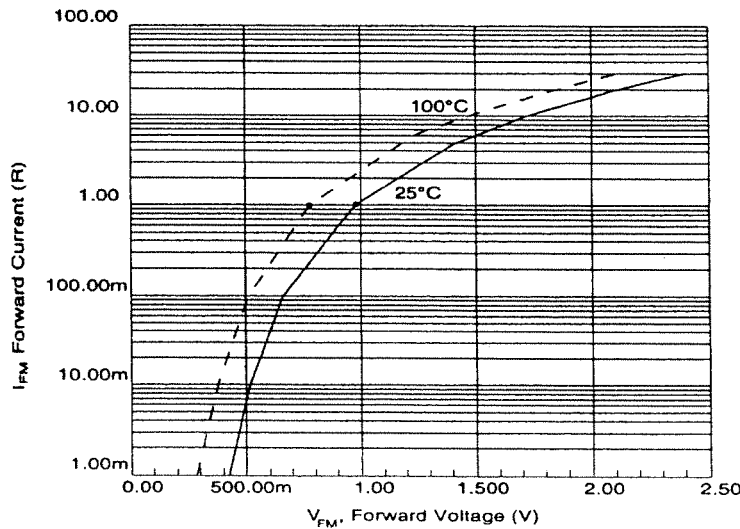


FIGURE 3.21 MURH840CT Forward-bias Voltage Temperature Characteristics.

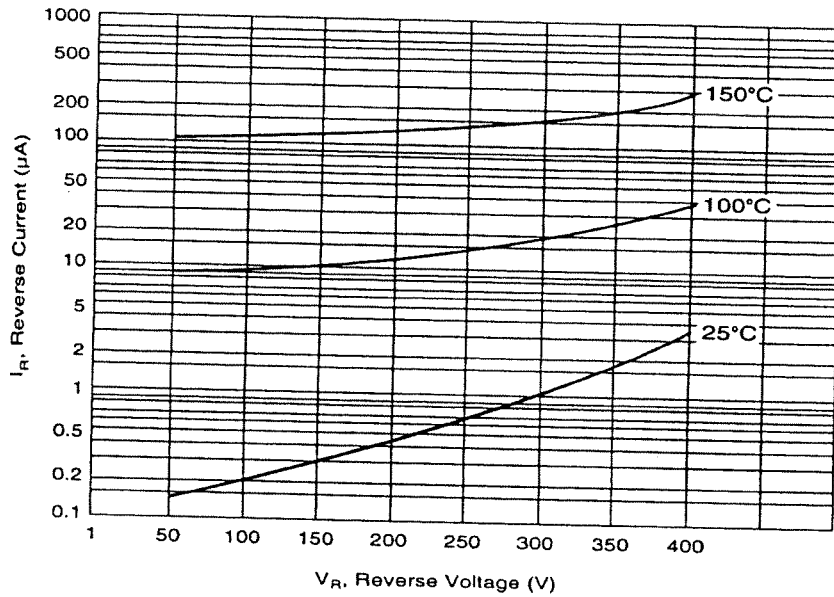


FIGURE 3.22 MURH840CT Reverse Leakage Current Temperature Characteristics.

2. *Method 3 (Reverse leakage current method).* In Figure 3.22, the reverse leakage current ( $I_R$ ) versus reverse voltage at three temperatures is plotted. At a reverse voltage of 400 V, the reverse currents at 25°C ( $T_o$ ) and 150°C ( $T_i$ ) are about 3.0  $\mu\text{A}$  ( $I_R(T_o)$ ) and 300.0  $\mu\text{A}$  ( $I_R(T_i)$ ), respectively. Again for EG of 1.11 eV, the value for the parameter XTI is computed from Equation 3.87 as

$$XTI = 3.710244 \quad (3.132)$$

In Table 3.9, the values of EG and XTI from each method are listed along with the diode voltage calculated at a current of 1.0 A for 27°C and 100°C, and the saturation current parameter IS calculated at 150°C. With the value of XTI obtained from Method 2, it is seen that the value of the TCV is close to that computed from the data sheet given in Equation 3.130. However, IS and, consequently,  $I_R$  calculated at 150°C is found to be much larger than the maximum value of  $I_R$  specified at this temperature which is 500  $\mu\text{A}$ . By using  $I_R$  data over temperature to extract XTI as was done with Method 3, IS at 150°C is found to be very close to  $I_R$  at the same temperature as shown in Figure 3.22. The value of the TCV computed with this XTI is, however, not as accurate that produced by the XTI of Method 2. Again, the specification for maximum  $I_R$  will be observed and XTI computed by Method 3 given in Equation 3.132 will be used.

### Reverse Breakdown Characteristics (BV, IBV)

The maximum dc blocking voltage  $V_R(\text{max})$  for this device is read from the data sheet as 400.0 V. Using a guard-band multiplier  $k_{BR}$  of 1.3, the breakdown voltage parameter BV is calculated from Equation 3.88 to be

$$BV = 520.0 \text{ V} \quad (3.133)$$

**TABLE 3.9** Comparison of Temperature Characteristics

Parameter or variable	Method		Units
	2	3	
EG	1.11	1.11	eV
XTI	23.702105	3.710244	
$V_F$ (27°C)	1.024041	1.024041	V
$V_F$ (150°C)	0.827068	0.966944	V
TCV	-2.698264	-0.782152	mV/°C
IS (150°C)	2.989445m	300.0	A

For a maximum simulation temperature of 150°C, the current at the breakdown voltage IBV is calculated from Equation 3.89 as

$$IBV = 4.279703 \text{ A} \quad (3.134)$$

## SUMMARY

To summarize the extraction process, all SPICE parameters for the MURH840CT are listed in Table 3.10. Characteristic plots generated by the SPICE diode model using these parameters are shown in Figures 3.23(a) through 3.23(d).

The SPICE diode model has been shown to consist of a set of equations and parameters derived from the theory developed for an ideal diode. Certain modifications of these equations allow the model added accuracy in the simulation of real diodes. Although the model has some limitations, it can be used to realistically model the behavior of most semiconductor *pn* junction devices which include low-current integrated circuit diodes, high-current rectifiers, varactor diodes, Zener diodes, and Schottky barrier diodes.

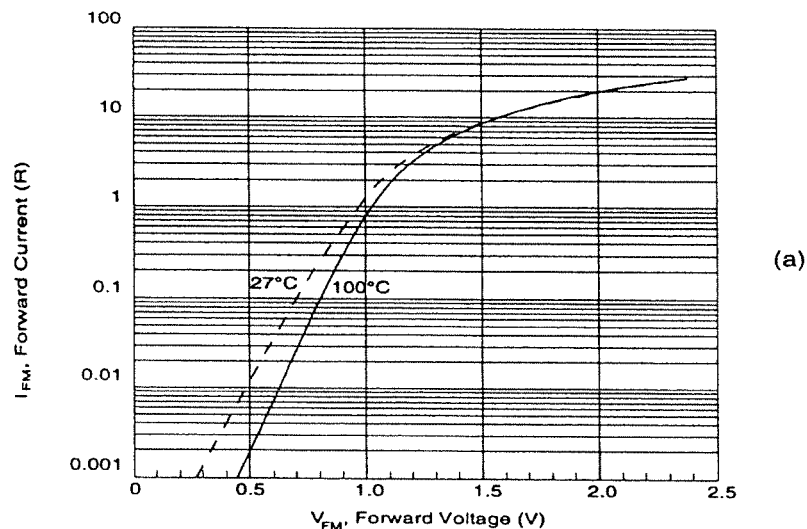


**FIGURE 3.23** (a) MURH840CT SPICE Model Forward Voltage DC Characteristics at 27°C and 100°C. (continued)

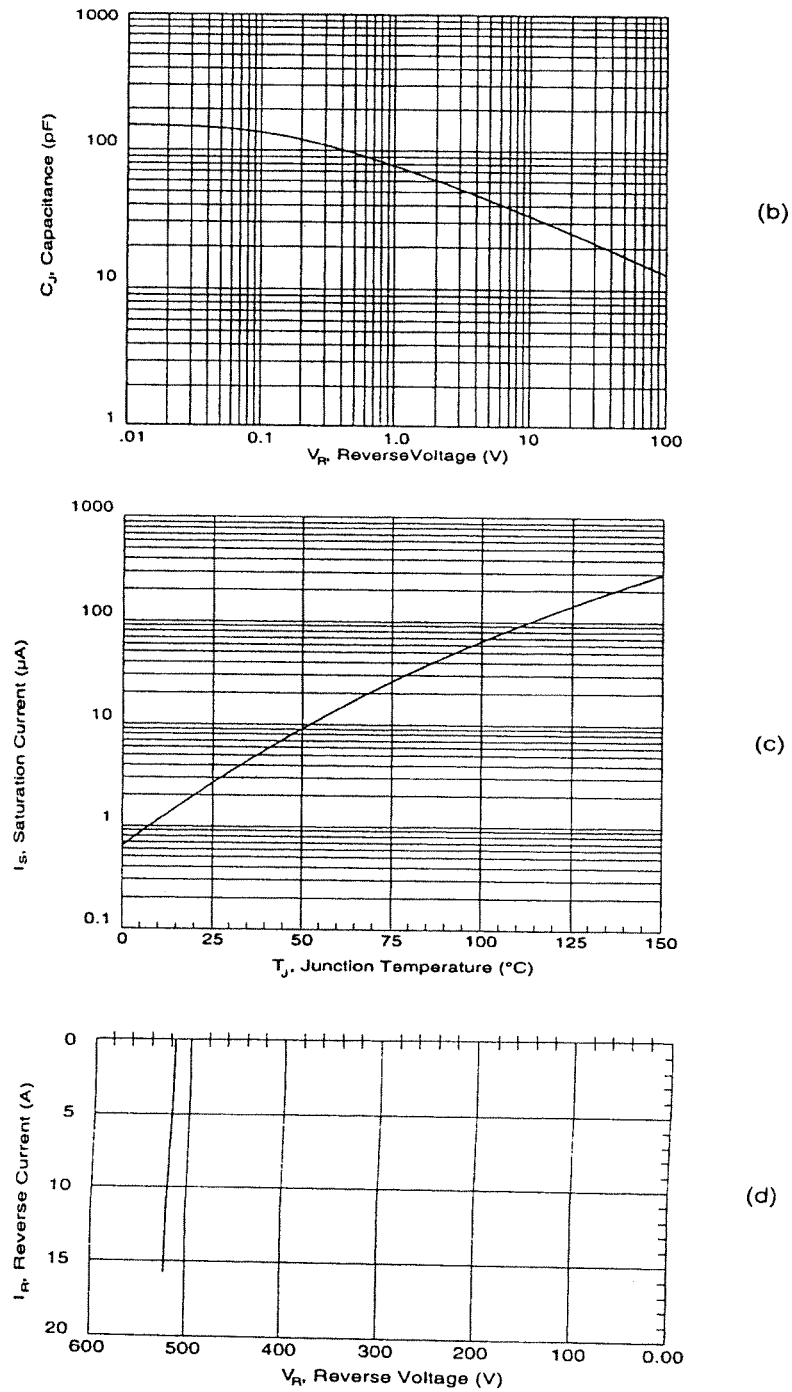


**FIGURE 3.23** (continued) (b) MURH840CT SPICE Model Reverse-bias C-V Characteristics; (c) MURH840CT SPICE Model Reverse Leakage Current Characteristics; (d) MURH840CT SPICE Model Reverse Breakdown Characteristics.

**TABLE 3.10** SPICE Diode Model Parameters for the MURH840CT

Name	Parameter	MURH840CT value	Units
IS	Saturation current	3.0 $\mu$	A
RS	Ohmic resistance	42.07777m	ohm
N	Emission coefficient	2.986477	
TT	Forward transit time	32.96688n	sec
CJO	Zero-bias junction capacitance	155.9821p	F
VJ	Contact potential	0.2159243	V
M	Junction capacitance grading exponent	0.4082637	
EG	Energy gap	1.11	eV
XTI	IS temperature exponent	3.710244	
KF	Flicker noise coefficient	0	
AF	Flicker noise exponent	1.0	
FC	CJ forward-bias coefficient	0.5	
BV	Reverse breakdown	520.0	V
IBV	Current at BV	4.279703	A

## References

1. A. S. Grove, *Physics and Technology of Semiconductor Devices*, John Wiley and Sons, Inc., New York, NY, 1967.
2. A. Bar-Lev, *Semiconductors and Electronic Devices*, Prentice-Hall International, Inc., London England, 1979.
3. R. S. Muller and T. I. Kamins, *Device Electronics for Integrated Circuits*, John Wiley and Sons, Inc., New York, NY, 1977.
4. B. G. Streetman, *Solid State Electronic Devices, Second Edition*, Prentice-Hall Inc., Englewood Cliffs, NJ, 1980.
5. *SPICE 2 User's Guide*, University of California Berkeley, Electronics Research Labs, Berkeley, CA.
6. P. Antognetti and G. Massobrio, *Semiconductor Device Modeling With SPICE*, McGraw-Hill Book Co., Inc., New York, NY, 1988.
7. C. F. Gerald, *Applied Numerical Analysis*, Addison-Wesley Publishing Co., Reading, MA, 1970.
8. B. Miller, "Curve Fitting Made Easy", *RF Design*, Vol. 13, No. 6, June 1990, pp. 27 to 32.
9. B. A. Leinfelder, "Improving PN Junction Reverse Recovery Measurements", *PCIM*, Part 1, January 1988, pp. 41 to 44; Part 2, February 1988, pp. 43 to 45; Part 3, March 1988, pp. 52 to 54.
10. *Rectifiers and Zener Diodes Data Book*, Technical Information Center, Motorola, Inc., 1987.